energies

MDPI

Article

China's Terrestrial Hydro-, Wind-, and Photovoltaic-Power Potentials and CO_2 Emission Reductions Under Different Development Scenarios

Bing Li [1,2,3], Mingwei Ma [4], Chongxu Zhao [2,3,*], Caihong Hu [1] and Liangyan Zhang [5]

[1] School of Water Conservancy and Transportation, Zhengzhou University, Zhengzhou 450001, China; libingyrihr@126.com (B.L.); hucaihong@zzu.edu.cn (C.H.)
[2] Yellow River Institute of Hydraulic Research, Zhengzhou 450003, China
[3] Key Laboratory of Yellow River, Ministry of Water Resources, Zhengzhou 450003, China
[4] College of Water Resources, North China University of Water Resources and Electric Power, Zhengzhou 450045, China; mamingwei@ncwu.edu.cn
[5] Nanjing Water Resources Management Center, Nanjing 210008, China; cindyliangyan@126.com
* Correspondence: charles_zcx@163.com

Abstract

This study evaluates the resource, technical, economic, and CO_2 mitigation potentials of terrestrial hydropower, wind power, and photovoltaic (PV) power in China under historical and future SSP(Shared Socioeconomic Pathways) climate scenarios. By integrating hydro-meteorological observations, land-use information, digital elevation data, nature-reserve constraints, and CMIP6 climate outputs, we estimate renewable-energy potentials through a consistent national-scale screening framework and cost–supply curve analysis. The results show clear spatial heterogeneity among the three energy sources. Hydropower potential is concentrated mainly in the Yangtze River basin, Pearl River basin, and Southwestern International Rivers. Wind-power potential is relatively high in northwestern, northeastern, and plateau regions, while PV potential is particularly large in northwestern, northern, northeastern, and selected southeastern regions. Under the adopted assumptions, PV shows the largest resource and technical potential, followed by wind power and hydropower; however, this ranking reflects resource potential rather than comprehensive deployment superiority. Practical development is also constrained by ecological flow requirements, land-use competition, grid integration, storage demand, transmission capacity, curtailment risk, and regional demand matching. The findings provide a national-scale comparative reference for renewable-energy planning and CO_2 mitigation, while highlighting the need for future work that incorporates dynamic land use, system-level integration costs, detailed turbine or power-curve modeling, and dynamic grid-emission factors.

Keywords: renewable energy potential; CO_2 emission reduction; SSP scenarios; climatic resources; cost and supply; China

Check for updates

Academic Editor: Jay Zarnikau

Received: 18 May 2026
Revised: 26 June 2026
Accepted: 28 June 2026
Published: 6 July 2026

Copyright: © 2026 by the authors. Licensee MDPI, Basel, Switzerland. This article is an open access article distributed under the terms and conditions of the Creative Commons Attribution (CC BY) license.

1. Introduction

The dramatic increase in energy consumption and the exacerbation of global warming through greenhouse gas emissions have made it imperative to decarbonize the global economy and accelerate the transition of the energy sector toward renewable sources [1–9]. Research indicates that to achieve the 2 °C warming target, over 30% of global oil reserves, 50% of natural gas reserves, and more than 80% of coal reserves must remain untapped by 2050 [10]. This necessitates a gradual reduction in reliance on conventional fossil fuels, an

accelerated shift toward renewable energy, and the implementation of measures to enhance energy efficiency and reduce carbon emissions [11–17]. Against this backdrop, it is evident that climate stabilization in the 21st century will inevitably depend on the advancement of renewable [18–23]. Currently, China is actively promoting sustainable energy development, integrating renewable energy as a key component of its national energy strategy, and has achieved significant progress in harnessing hydropower, wind, and solar energy [24].

Hydropower, recognized for its environmental sustainability, stability, and cost-effectiveness, has been extensively developed and utilized worldwide. Numerous studies have examined potential alterations in hydropower resource endowments under climate change from hydrological perspectives [25–29]. For instance, Fan et al. [30] investigated precipitation impacts on hydropower generation under climate change, demonstrating that a 1% increase in precipitation elevates hydropower output by 0.081%. Lehner et al. [31] developed a WaterGAP-based methodology, projecting up to 25% or greater reductions in hydropower potential across European nations due to climate change. Wang et al. [32] analyzed long-term precipitation–hydropower relationships, employing gray models to predict precipitation trends; their findings indicate heightened vulnerability of hydropower resources in southwestern China under high-emission scenarios. Concurrently, research has evaluated climate change impacts on hydropower systems through socioeconomic and electricity market lenses. Evidence suggests climate change serves as a pivotal driver of renewable energy development [33,34]. However, hydropower generation may experience either positive [35] or negative [36] climate-induced effects across different regions.

As a crucial component of renewable energy systems, wind power is poised to play an increasingly pivotal role in facilitating the clean energy transition and mitigating carbon emissions [37,38]. However, the potential impacts of climate change on wind energy resources remain incompletely understood due to uncertainties in meteorological parameter alterations and climate variability [39–44]. Davidson et al. [45] demonstrated that through proactive power sector reforms at current feed-in tariff levels, grid-connected wind power could contribute approximately 26% of total electricity supply by 2030, thereby substantially supporting China's target of achieving 20% non-fossil energy in primary energy consumption. Conversely, Sherman et al. [46] identified a declining trend in wind-power potential for China's traditionally wind-rich Inner Mongolia region through analysis of historical wind patterns. Feng et al. [47] further quantified China's onshore technical wind energy potential, revealing a range of 2560 to 3501 TWh/yr depending on agricultural land-use constraints (0% versus 70% utilization scenarios).

Photovoltaic (PV) power generation represents a critical pathway for solar energy utilization, offering substantial carbon emission reductions that are instrumental in achieving global temperature control targets and China's dual carbon goals of peak emissions and carbon neutrality [48–50]. Extensive international research has investigated climate impacts on solar radiation resources [51], and solar power generation [52], with particular emphasis on PV generation potential [53–57]. China-specific studies have yielded significant findings in this domain [58,59]. He and Kammen [60] conducted a comprehensive provincial assessment of solar availability using hourly irradiance data from 200 representative locations (2001–2010), revealing distinct spatiotemporal variations in China's solar resources. Chen et al. [61] quantified concentrated solar power potential at the provincial level, estimating installable capacity of 2.45×10^7 to 5.40×10^7 MW with corresponding annual generation potential of 6.46×10^{13} to 1.85×10^{14} kWh. Furthermore, Chen et al. [62] evaluated the Belt and Road Initiative region's technical PV potential, demonstrating an annual generation capacity of 448.9 PWh, equivalent to 41.3 times the region's 2016 electricity demand.

Although numerous studies have assessed individual renewable-energy resources in China, comprehensive comparisons of terrestrial hydropower, wind power, and PV power

under a unified national-scale framework remain limited, particularly when future climate scenarios and CO_2 mitigation implications are considered together. Existing studies often focus on a single energy source, a specific region, or a specific technical pathway, making it difficult to compare resource endowments, spatial constraints, economic potential, and mitigation implications across multiple renewable-energy types using consistent assumptions. Moreover, the practical interpretation of large theoretical or technical potentials is often insufficiently discussed, especially with respect to land-use constraints, grid integration, storage demand, transmission bottlenecks, and regional demand matching.

The objective of this study is therefore to provide a comparative national-scale assessment of terrestrial hydropower, wind power, and PV power potentials and their associated CO_2 emission-reduction capacities in China under historical and future SSP scenarios. Specifically, this study addresses three research questions: (1) How are the geographic, technical, and economic potentials of hydropower, wind power, and PV power distributed across China's major river basins and provinces? (2) How do these potentials and their associated CO_2 mitigation capacities vary under different future climate scenarios? (3) How should the estimated resource and technical potentials be interpreted when practical deployment constraints, such as ecological protection, land-use competition, grid integration, storage, and transmission, are considered?

The novelty of this study lies in integrating multiple renewable-energy resources into a consistent national-scale assessment framework, comparing their spatial patterns under SSP-based climate conditions, and jointly evaluating their generation potential and CO_2 mitigation implications. First, the theoretical potential of each energy source is calculated from climatic and hydrological data. Geographic and technical constraints are then applied to derive geographic and technical potentials. The technical potential is further combined with simplified generation-side cost assumptions to construct cost–supply curves and estimate economic potential. Finally, grid emission factors are used to estimate CO_2 emission reductions. The results are interpreted as national-scale screening estimates rather than immediately deployable capacity.

2. Materials and Methods

2.1. Study Area

China is situated in eastern Asia along the western Pacific coast, spanning longitudes 73°33′ to 135°05′ E and latitudes 18°10′ to 53°33′ N (Figure 1). This vast territory exhibits diverse topography and climatic characteristics. The western regions are dominated by high mountains and plateaus, where the alpine climate significantly influences water resources and energy production. In contrast, the eastern and southern areas consist mainly of hills and plains, supporting dense populations and industrial activities, making them the most economically developed zones and the primary consumers of water and energy resources. Due to variations in terrain, climate, and geographical conditions, the hydrological characteristics of China's major river basins display considerable diversity and complexity. For the study of hydropower potentials, this paper divides China's land area into eleven major river basins (Figure 1a). In contrast, wind and solar PV power potentials are analyzed at the provincial scale (Figure 1b).

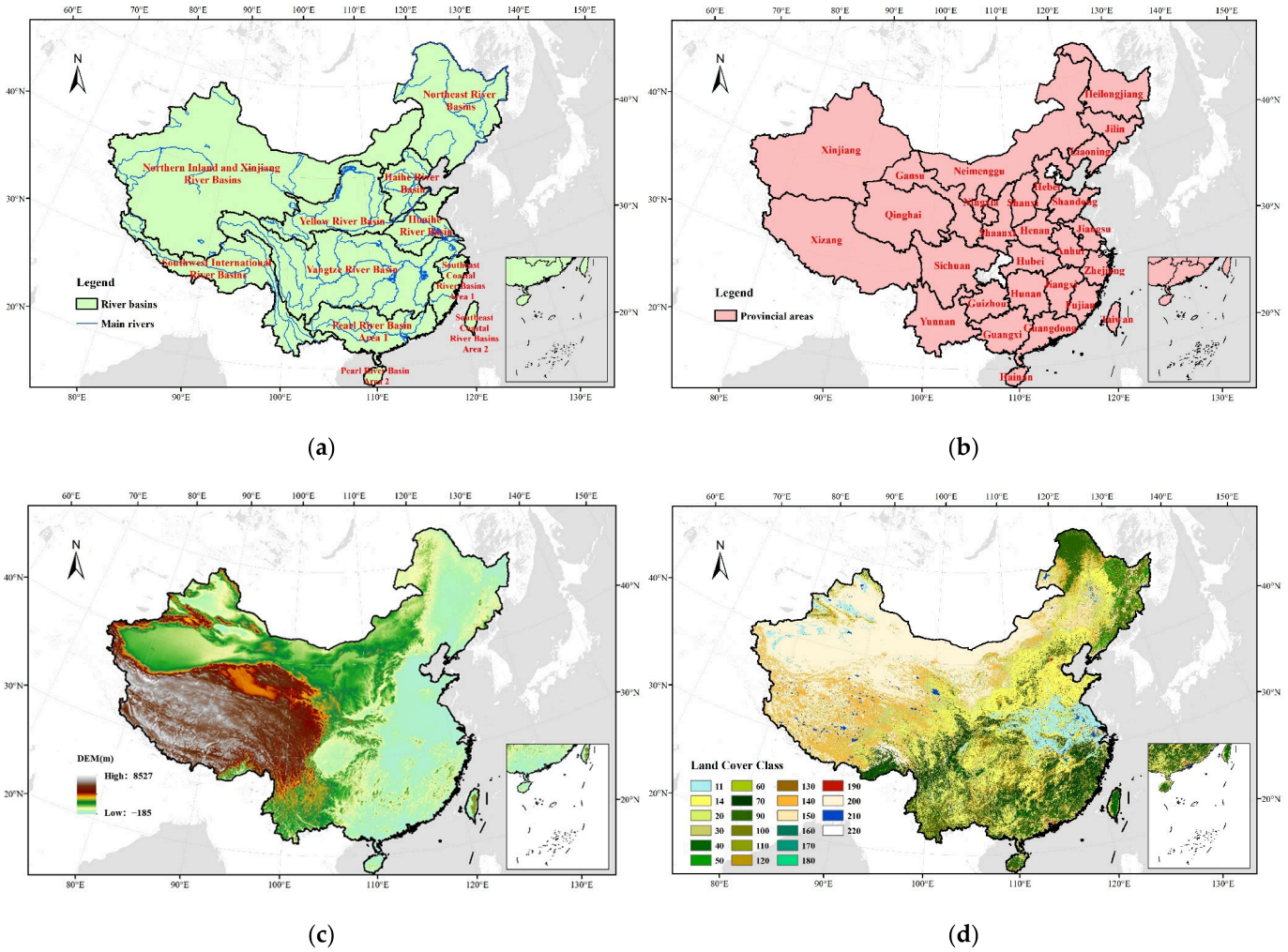


Figure 1. Research subareas and geographical features of terrestrial China: (**a**) river basins, (**b**) provincial areas, (**c**) DEM, and (**d**) land cover.

2.2. Data Sources and Preprocessing

The datasets employed in this study encompass historical meteorological and hydrological records, digital elevation models, land-use data, nature reserve distributions, and outputs from global climate models across China's terrestrial domain, with detailed descriptions provided in Table 1. The climate model simulations were downscaled using the Delta method and spatially interpolated to a 0.5° × 0.5° resolution via inverse distance weighting (IDW). Subsequently, bias correction was performed using the Equidistant Cumulative Distribution Functions (EDCDF) method. Building upon these processed datasets, the study applied the following methodology to estimate the geographic, technical, and economic potentials of hydropower, wind power, and photovoltaic power generation, and associated CO_2 emission reductions.

2.3. Workflow of Renewable-Energy Potential Assessment

Figure 2 presents the overall workflow of this study. First, historical observations, CMIP6 climate-model outputs, DEM data, land-cover data, and nature-reserve information were collected and preprocessed. Second, geographic suitability screening was performed separately for hydropower, wind power, and PV power according to their resource and spatial requirements. Third, geographic and technical potentials were estimated using energy-specific equations and conversion assumptions. Fourth, simplified generation-side LCOE assumptions were used to construct cost–supply curves and estimate economic po-

tentials. Finally, CO_2 emission reductions were estimated by combining technical potentials with grid emission factors. The resulting potentials were then compared across energy types, regions, and scenarios, with explicit discussion of assumptions and limitations.

Table 1. Details about the data used in this study.

Data Type	Period	Temporal Resolution	Spatial Resolution	Data Source and Website	Data Description
Historical meteorological and hydrological data	1961–2022	Daily	0.1°	NOAA National Centers for Environmental Information (NCEI) https://www.ncei.noaa.gov/products/geomagnetic-data (accessed on 7 May 2026)	Mainly including wind speed (m/s), temperature (°C), runoff, (mm) and solar irradiance (W/m^2). Daily observations reorganized into annual data.
Digital elevation model (DEM) data	2008	–	90 m	Hydrological data and maps based on SHuttle Elevation Derivatives at multiple Scales (HydroSHEDS) https://www.hydrosheds.org/products/hydrosheds (accessed on 7 May 2026)	The HydroSHEDS database offers a suite of global digital data layers, including various hydrographic products (e.g., DEM, flow direction and accumulation) at multiple resolutions and scales.
Land use/cover data	2009	–	300 m	European Space Agency https://due.esrin.esa.int/page_globcover.php (accessed on 7 May 2026)	ESA's 2009 global land cover map (GlobCover 2009), validated using more than 3000 reference land cover points and classified global land use/cover into 22 categories.
Nature reserves data	2021	–	–	Star Map Cloud Open Platform https://open.geovisearth.com/ (accessed on 7 May 2026)	Distribution map of China's terrestrial nature reserves (areal vector data).
CMIP6 GCMs data	Historical (1961–2014) Future (2030–2100)	Daily	0.5°	China Meteorological Administration National Climate Center https://data.cma.cn/ (accessed on 7 May 2026)	Three CMIP6 GCMs (ACCESS-ESM1-5, BCC-CSM2-MR, and FGOALS-f3-L) with four selected scenarios (historical, SSP126, SSP245, and SSP585). Daily outputs reorganized into annual data.

2.4. Hydropower Energy

2.4.1. Modeling of Possible Power Plants

For assessing hydropower potentials, this study first assumes all rivers remain in their undeveloped state, excluding areas adjacent to large water bodies such as lakes and wide shallow rivers. Secondly, to safeguard navigation and related functions, regions within 200 km upstream of river outlets with depths exceeding 4 m are excluded. Furthermore, to maintain ecological processes (e.g., fish migration), it is assumed that hydropower stations release at least 30% of the natural discharge. Using these assumptions, the HydroSHEDS DEM and flow direction data are first utilized to derive the hydrological distance from each grid cell to the basin outlet along the downstream flow path, generating a hydrological

distance map. Subsequently, starting from the basin outlet and progressing upstream, distances are systematically allocated, and potential hydropower stations are identified at 30 km intervals along river segments based on runoff data. Finally, existing hydropower stations are incorporated to optimize the simulated potential sites, avoiding duplicate calculations of overlapping reservoirs. Through these procedures, a total of 1065 simulated hydropower sites are identified across China's terrestrial area, as illustrated in Figure 3.

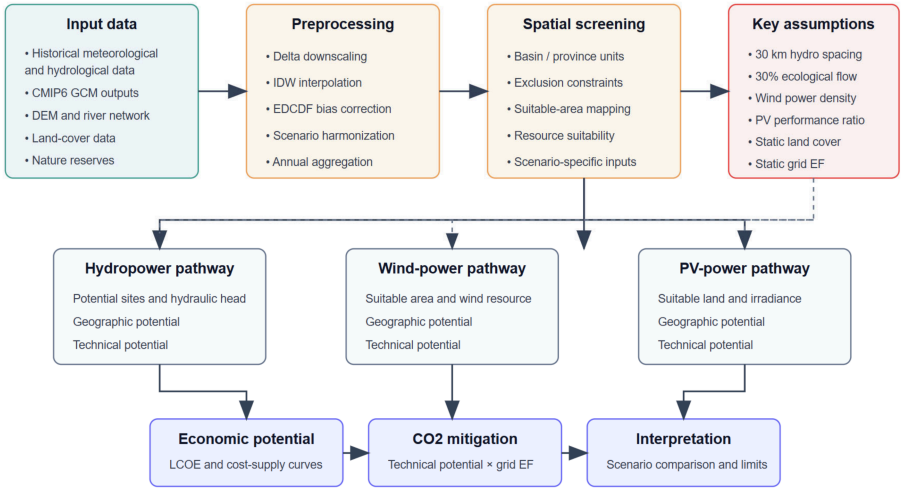


Figure 2. Workflow for assessing hydropower, wind-power, and PV power potentials and CO_2 emission reductions under historical and future SSP scenarios.

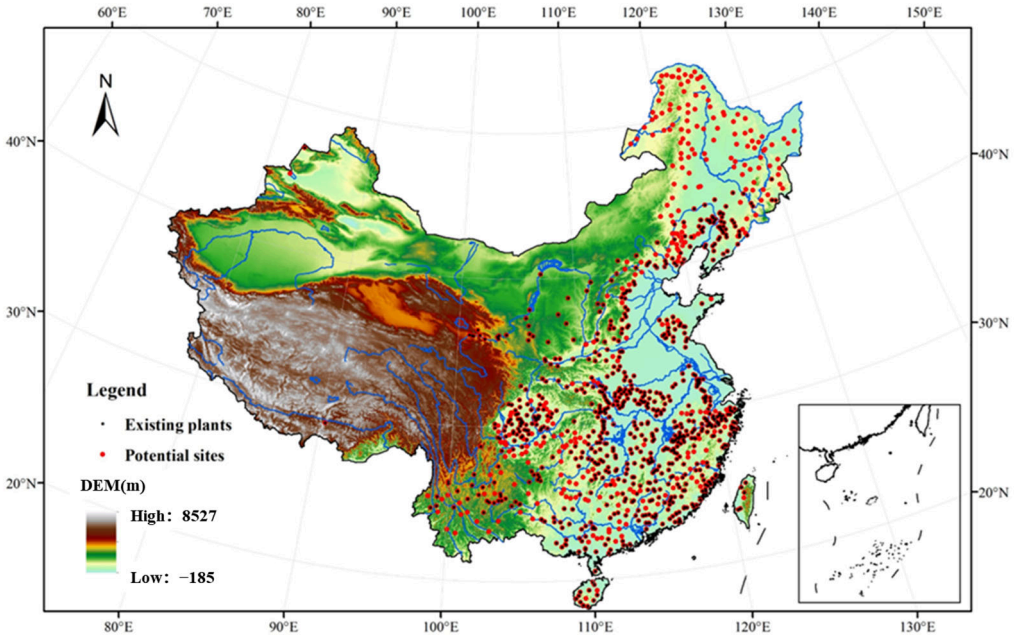


Figure 3. Simulation results of potential hydropower plants in China.

2.4.2. Geographic Potential Estimation of Hydropower Stations

The geographical potential of hydropower stations can be estimated as [63]:

$$E_{G,Wa} = \rho \times g \times \left(Z_1 - Z_2 - h_f\right) \times Q \times T \times 10^{-15} \quad (1)$$

where $E_{G,Wa}$ represents hydropower geographical potential, PWh; ρ is water density, kg/m^3; g is gravitational acceleration, 9.8 m/s^2; Z_1 and Z_2 are, respectively, water intake

and power station elevation, m; h_f denotes head loss, m; Q indicates designed water diversion flow rate, m^3/s; and T represents time, h.

2.4.3. Technical Potential Estimation of Hydropower Stations

The technical potential of hydropower is derived from geographical potential and corresponding efficiency, estimated as follows:

$$E_{T,Wa} = \rho \times g \times \left(Z_1 - Z_2 - h_f\right) \times Q \times T \times \eta \times 10^{-15} \quad (2)$$

where $E_{T,Wa}$ represents hydropower technical potential, PWh; η denotes turbine efficiency, which is a function of the flow rate Q and typically ranges between 0.7 and 0.9; and all other symbols retain their previously defined meanings.

2.5. Wind-Power Potential Assessment

2.5.1. Geographic Analysis and Assessment of Wind-Power Generation

First, areas unsuitable for wind farm development are excluded, such as permanent snow-covered regions and steep mountainous areas. Second, care is taken to ensure that wind farm construction does not significantly disrupt existing land-use functions, such as agricultural production. Third, suitability constraints are applied to the remaining land area to determine the most favorable locations for wind-power projects. In this study, topographic and geomorphological data for each province are collected and analyzed, including the distribution of mountain ranges and plains (Figure 4). Meteorological data, land-use types, and wind energy resources are then integrated to conduct a GIS-based suitability assessment. Through this analysis, geographic constraint factors for wind-power generation are derived, which comprehensively reflect provincial suitability based on topography, land cover, and climatic conditions (Table 2). Based on this assessment, the geographic, technical, and economic potentials of onshore wind-power generation, along with corresponding CO_2 emission reductions, are estimated for each province in China.

Table 2. The geographical limiting factor for wind-power energy in each province of China.

Province	**Hunan**	**Taiwan**	**Hainan**	**Yunnan**	**Guangdong**	**Fujian**	**Guizhou**
Factor	0.663	0.631	0.607	0.603	0.622	0.602	0.587
Province	**Jiangxi**	**Zhejiang**	**Sichuan**	**Hubei**	**Anhui**	**Jiangsu**	**Qinghai**
Factor	0.594	0.690	0.588	0.612	0.681	0.830	0.638
Province	**Gansu**	**Shaanxi**	**Shanxi**	**Henan**	**Hebei**	**Shandong**	**Liaoning**
Factor	0.622	0.592	0.580	0.738	0.740	0.768	0.751
Province	**Jilin**	**Heilongjiang**	**Xizang**	**Guangxi**	**Neimenggu**	**Ningxia**	**Xinjiang**
Factor	0.720	0.710	0.400	0.552	0.487	0.571	0.688

2.5.2. Geographic Potential Estimation of Wind-Power Generation

The geographical potential of wind-power generation was estimated using a simplified wind-resource intensity framework [64,65]:

$$E_{G,Wi} = A \times P_{wi} \times h \times E_\eta \times 10^{-9} \quad (3)$$

where $E_{G,Wi}$ denotes wind-power geographical potential, PWh; A represents suitable area for wind-power generation, km^2; P_{wi} is the wind-power density or wind-resource intensity term derived from wind-speed information (W/m^2); h denotes number of hours in a year (8760 h); and E_η is geographical constraint factor.

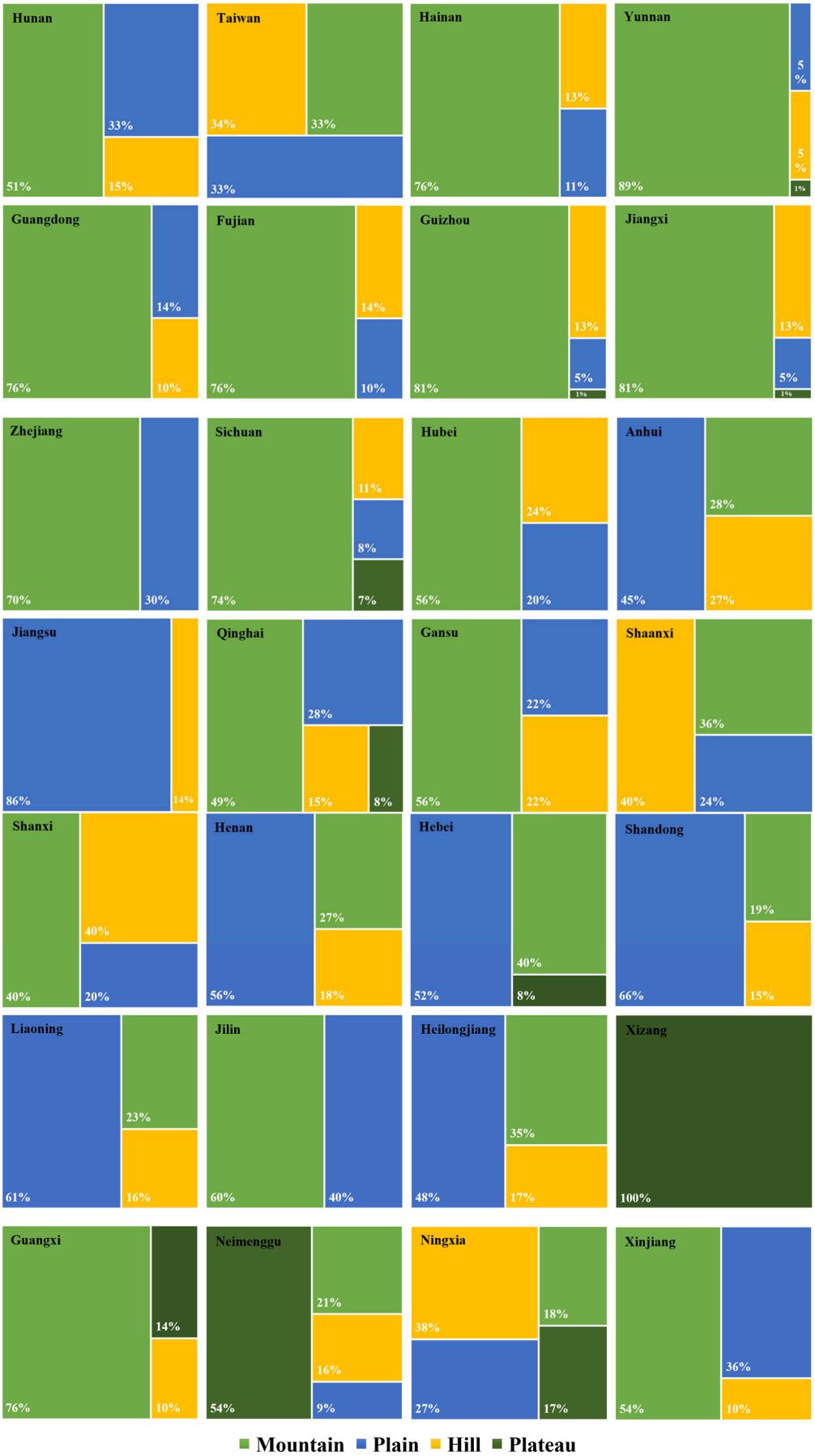


Figure 4. Geomorphic information at the provincial scale in China.

2.5.3. Technical Potential Estimation of Wind-Power Generation

The technical potential of wind-power generation can be estimated using the following formula:

$$E_{T,Wi} = A \times \eta_a \times \eta_{ar} \times D \times h_f \times 10^{-9} \quad (4)$$

where $E_{T,Wi}$ represents wind-power technical potential, PWh; η_a denotes annual availability factor accounting for wind turbine maintenance, taken as 95% in this study; η_{ar} is the wind farm array efficiency, assumed to be 90%; D refers to the power density, set to 4 MW/km^2; and h_f indicates the full-load hours, h.

The wind-power assessment in this study is intended for national-scale resource screening rather than turbine-level energy-yield simulation. Regional wind-resource differences are represented through the wind-resource intensity term, geographic screening, suitability constraints, and full-load-hour assumptions. This simplified framework supports comparison among hydropower, wind power, and PV power under consistent national assumptions, but it does not explicitly resolve turbine-level aerodynamic conversion, hub-height correction, Weibull wind-speed distributions, cut-in/cut-out speeds, or manufacturer-specific power curves. Therefore, the wind-power results should be interpreted as broad regional screening estimates. Future work should incorporate turbine power curves and wind-speed distributions to refine the physical representation of wind-energy conversion.

2.6. PV Power Potential Assessment

2.6.1. Geographic Analysis and Assessment of PV Power Generation

Photovoltaic (PV) power generation potential, similar to wind power, depends on multiple factors, including climatic conditions, topography, and land-use characteristics. This study first determines geographically suitable areas for PV generation using GIS technology and provincial surface data presented in Figure 4. Then, terrestrial nature reserve areas are excluded to preserve their critical role in maintaining ecological balance. Additionally, land types unsuitable for PV installation are systematically filtered out. The GlobCover 2009 dataset identifies land-cover types with classification values of 30 (mosaic vegetation), 140 (closed to open grasslands), 150 (sparse vegetation), and 200 (bare areas) as suitable for PV deployment. In contrast, the remaining 18 land-cover types, including croplands, dense vegetation, water bodies, and snow-covered regions, are considered unsuitable (see Table 3 for details). This comprehensive geographical analysis and evaluation yields the final suitable terrestrial areas for PV development in China, as represented in Figure 5.

Table 3. The correspondence of land-cover class value (label) and description defined in GlobCover 2009.

No.	Value (Label)	Land Cover Class Description
1	11	Post-flooding or irrigated croplands (or aquatic)
2	14	Rainfed croplands
3	20	Mosaic cropland (50–70%)/vegetation (grassland/shrubland/forest) (20–50%)
4	30	Mosaic vegetation (grassland/shrubland/forest) (50–70%)/cropland (20–50%)
5	40	Closed to open (>15%) broadleaved evergreen or semi-deciduous forest (>5 m)
6	50	Closed (>40%) broadleaved deciduous forest (>5 m)
7	60	Open (15–40%) broadleaved deciduous forest/woodland (>5 m)
8	70	Closed (>40%) needleleaved evergreen forest (>5 m)
9	90	Open (15–40%) needleleaved deciduous or evergreen forest (>5 m)
10	100	Closed to open (>15%) mixed broadleaved and needleleaved forest (>5 m)
11	110	Mosaic forest or shrubland (50–70%)/grassland (20–50%)
12	120	Mosaic grassland (50–70%)/forest or shrubland (20–50%)

Table 3. *Cont.*

No.	Value (Label)	Land Cover Class Description
13	130	Closed to open (>15%) (broadleaved or needleleaved, evergreen or deciduous) shrubland (<5 m)
14	140	Closed to open (>15%) herbaceous vegetation (grassland, savannas or lichens/mosses)
15	150	Sparse (<15%) vegetation
16	160	Closed to open (>15%) broadleaved forest regularly flooded (semi-permanently or temporarily)—Fresh or brackish water
17	170	Closed (>40%) broadleaved forest or shrubland permanently flooded—Saline or brackish water
18	180	Closed to open (>15%) grassland or woody vegetation on regularly flooded or waterlogged soil—Fresh, brackish or saline water
19	190	Artificial surfaces and associated areas (Urban areas > 50%)
20	200	Bare areas
21	210	Water bodies
22	220	Permanent snow and ice
23	230	No data (burnt areas, clouds, etc.)

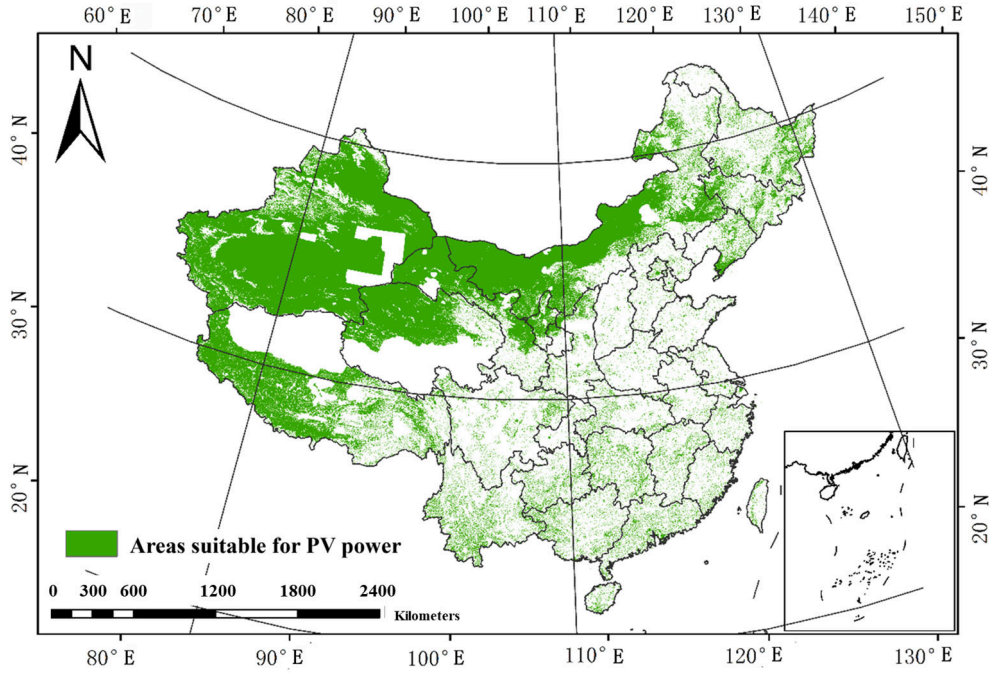


Figure 5. Areas suitable for photovoltaic power generation in China.

2.6.2. Geographic Potential Estimation of PV Power Generation

The geographical potential of PV power generation can be estimated as follows [64,65]:

$$E_{G,Pv} = I \times h \times A \times f \times 10^{-9} \quad (5)$$

where $E_{G,Pv}$ represents geographical potential of PV power generation, PWh; I denotes solar irradiance, W/m^2; h is number of hours in a year (8760 h); A corresponds to the suitable land area for PV development, km^2; and f is the suitability factor. The factor 10^{-9} converts W/m^2 × h × km^2 to PWh, because 1 km^2 = 10^6 m^2 and 1 PWh = 10^{15} Wh.

2.6.3. Technical Potential Estimation of PV Power Generation

The technical potential of PV power generation can be obtained as:

$$E_{T,Pv} = E_{G,Pv} \times u_{Pv} \times pr \quad (6)$$

where $E_{T,Pv}$ denotes technical potential of PV power generation, PWh; u_{Pv} is the effective land-area utilization coefficient for PV deployment; and pr stands for performance ratio, assumed to be 85% in this study. In this study, u_{Pv} is 0.764, as derived from the ratio between the reported technical and geographical PV potentials after accounting for pr. This coefficient should not be interpreted as the PV module or cell conversion efficiency. Instead, it represents the proportion of suitable land area effectively occupied by PV arrays after considering site-layout requirements such as row spacing, access roads, inverter and substation footprints, and other land-use constraints. To avoid ambiguity, the expression 'PV panel utilization efficiency' has been replaced by 'effective land-area utilization coefficient'.

2.7. Key Assumptions and Interpretation of Potentials

This study is designed as a national-scale screening assessment rather than a project-level feasibility study. Therefore, several assumptions are required to ensure consistency among energy types, regions, and climate scenarios. These assumptions influence the absolute magnitude of the estimated potentials and should be considered when interpreting the results. The geographic and technical potentials reported in this study represent resource availability under the adopted screening criteria; they should not be interpreted as immediately deployable capacity.

Table 4 summarizes the main assumptions used in the assessment and their interpretation. For hydropower, the 30 km interval for potential site identification provides a standardized spacing rule for national-scale river-network screening, while the 30% ecological-flow release and the exclusion of downstream river-mouth sections are used to avoid overestimating exploitable potential in ecologically and navigationally sensitive river segments. For wind power, the current assessment uses a simplified power-density and full-load-hour framework. This framework is suitable for broad regional comparison but does not replace detailed turbine-level modeling based on hub-height correction, Weibull wind-speed distributions, cut-in/cut-out speeds, or turbine power curves. For PV power, suitable land-cover classes were identified using GlobCover 2009 and nature-reserve constraints. Because dynamic land-use change is not represented, PV suitable areas should be interpreted as a static baseline estimate. CO_2 mitigation estimates use static grid emission factors, which may overestimate future avoided emissions if China's power system continues to decarbonize.

2.8. Economic-Potential Estimation and LCOE Assumptions

The technical potential is treated as the annual energy output (i.e., energy supply), measured in kWh. By dividing the annualized investment cost by the energy supply quantity, the levelized cost of electricity (LCOE) can be obtained, expressed in Yuan·kWh^{-1}. These discrete cost–supply sequences are then sorted in ascending order to generate the corresponding cost–supply curves (as illustrated in Figure 6). Throughout this study, this curve method is employed to quantify the economic potential of hydro-, wind-, and photovoltaic-power under specified economic constraints (e.g., an LCOE of 0.4 Yuan/kWh).

The LCOE for hydropower generation can be estimated as:

$$LCOE_{Wa} = \frac{I_C + I_B + I_O + I_E}{E_{T,Wa} \times 10^{12}} \quad (7)$$

where $LCOE_{Wa}$ denotes LCOE of hydropower generation, Yuan/kWh; I_C is capital investment cost, Yuan; I_B is engineering construction cost, Yuan; I_O is operation and maintenance cost, Yuan; and I_E is environmental externalities cost, Yuan.

Table 4. Key assumptions and interpretation of estimated potentials.

Component	Baseline Treatment in This Study	Interpretation and Limitation	Expected Influence If Changed
Hydropower site interval	Potential sites identified at 30 km intervals along river segments	National-scale screening rule; not a project-level dam-siting design	Shorter spacing may increase potential sites but may also overestimate feasible development
Ecological flow	At least 30% of natural discharge reserved	Represents a simplified ecological-flow constraint	Higher ecological-flow release reduces hydropower potential
River-mouth exclusion	River sections within 200 km upstream of outlets with depth > 4 m excluded	Avoids overestimating development in navigation-sensitive downstream reaches	Smaller exclusion may increase potential but may reduce navigational/ecological realism
Wind technical potential	Power-density/full-load-hour framework; power density set to 4 MW/km^2	Simplified regional screening; turbine-level power curves are not explicitly modeled	Higher power density increases estimated technical potential nearly proportionally
PV technical potential	u_{Pv} assumed to be 0.764 and pr assumed to be 85%	u_{Pv} is an effective land-area utilization coefficient rather than module conversion efficiency; pr represents system performance losses	Larger u_{Pv} or pr increases estimated PV technical potential nearly proportionally
Land-cover screening	GlobCover 2009 and nature-reserve constraints	Static national land-cover baseline; recent land-use change not dynamically represented	Updated land cover may alter PV suitable area and regional distribution
CO_2 mitigation	Static grid emission factors	Avoided emissions may decline as the grid decarbonizes	Declining grid emission factors reduce future mitigation estimates

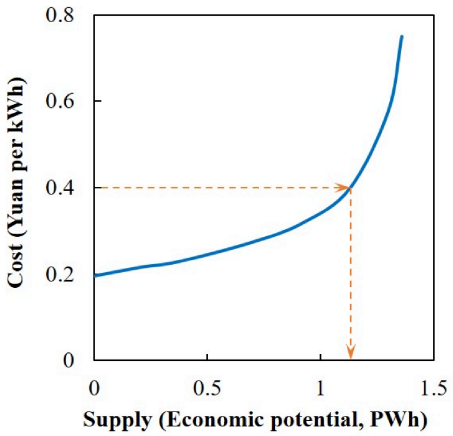


Figure 6. Illustration of the cost–supply curve and energy economic potential.

The LCOE for wind-power generation can be calculated using the following formula:

$$LCOE_{Wi} = \frac{\gamma(1+\alpha)I \cdot D}{E_{T,Wi} \times 10^{12}} \quad (8)$$

where $LCOE_{Wi}$ represents LCOE of wind-power generation, Yuan/kWh; I denotes total investment cost, Yuan; γ is annuity factor; and α indicates operation and maintenance cost factor, defined as a fixed percentage of investment cost and incorporated into annuity.

In this study, the annual operation and maintenance cost is assumed constant at 3% of investment cost (i.e., α = 0.03).

The LCOE for PV power generation is estimated using the following equation:

$$LCOE_{Pv} = \frac{\gamma(M+B) + \alpha(M+B)}{E_{T,Pv} \times 10^{12}} \quad (9)$$

where $LCOE_{Pv}$ represents LCOE of PV power generation, Yuan/kWh; γ denotes annuity factor; M indicates investment cost of PV modules, Yuan/m^2; B corresponds to balance of system (BOS) cost, which excludes grid connection but includes installation expenses, Yuan/m^2; and α signifies annual operation and maintenance cost expressed as a percentage of total investment costs, assumed to be 3% in this study.

The LCOE values in this study are interpreted as simplified generation-side cost estimates for constructing national-scale cost–supply curves. They are not intended to represent full system costs. Unless otherwise stated, the calculation accounts for technology-specific investment and operation costs through an annualized-cost framework, while storage, curtailment management, long-distance transmission expansion, detailed grid-connection reinforcement, and regional market heterogeneity are not included in the current estimate.

The economic-potential analysis in this study is intended as a national-scale generation-side screening assessment rather than a project-level techno-economic model. To improve transparency, Table 5 summarizes the fixed numerical assumptions, unit-conversion factors, and input cost terms used in the simplified LCOE framework. Fixed assumptions are listed explicitly, whereas cost terms that vary by hydropower site or province are identified as input variables in the LCOE equations. Therefore, the cost–supply curves should be interpreted as screening-level estimates for comparing relative economic potential across regions and scenarios, rather than as fully reproducible project-finance calculations for individual sites or provinces.

Table 5. Fixed assumptions, input cost terms, and reproducibility boundary of the simplified generation-side LCOE framework.

Item	Value or Treatment in This Study	Role in LCOE Calculation	Reproducibility Boundary
LCOE threshold for economic potential	0.4 Yuan/kWh	Used as the cost threshold for identifying economic potential from cost-supply curves	Fixed value reported in the manuscript
Wind installation density	4 MW/km^2	Used in wind technical-potential calculation	Fixed numerical assumption
Wind turbine availability factor	95%	Used in wind technical-potential calculation	Fixed numerical assumption
Wind-farm array efficiency	90%	Used in wind technical-potential calculation	Fixed numerical assumption
Wind O&M rate	3% of investment cost	Used in wind LCOE calculation	Fixed numerical assumption
PV performance ratio	85%	Used in PV technical-potential calculation	Fixed numerical assumption
PV O&M rate	3% of total investment cost	Used in PV LCOE calculation	Fixed numerical assumption
Hydropower technical potential	$E_{T,Wa}$ from Equation (2)	Denominator of hydropower LCOE	Derived from hydropower potential calculation
Wind technical potential	$E_{T,Wi}$ from Equation (4)	Denominator of wind LCOE	Derived from wind technical-potential calculation
PV technical potential	$E_{T,Pv}$ from Equation (6)	Denominator of PV LCOE	Derived from PV technical-potential calculation

Table 5. *Cont.*

Item	Value or Treatment in This Study	Role in LCOE Calculation	Reproducibility Boundary
Hydropower capital and construction costs	IC and IB	Numerator of hydropower LCOE	Site-specific input cost terms; complete site-level cost database is not provided
Hydropower O&M and environmental costs	IO and IE	Numerator of hydropower LCOE	Site-specific input cost terms; complete site-level cost database is not provided
Wind investment cost	I	Numerator of wind LCOE	Province- or scenario-specific input cost term; complete cost database is not provided
PV module and BOS costs	M and B	Numerator of PV LCOE	Input cost terms; complete cost database is not provided
Grid connection	Not explicitly itemized; PV BOS excludes grid connection	Not included in current generation-side LCOE	System-level cost excluded
Storage	Not included	Not included in current generation-side LCOE	System-level cost excluded
Curtailment management	Not included	Not included in current generation-side LCOE	System-level cost excluded
Long-distance transmission expansion	Not included	Not included in current generation-side LCOE	System-level cost excluded
Financing heterogeneity and regional market conditions	Not explicitly modeled	Not included in current generation-side LCOE	Discussed as limitation and future research
Unit conversion for hydropower potential	10^{-15}	Converts Wh to PWh in hydropower potential equations	Explicit conversion factor
Unit conversion for wind technical potential	10^{-9}	Converts MWh to PWh in wind technical-potential equation	Explicit conversion factor
Unit conversion for PV geographic potential	10^{-9}	Converts $W/m^2 \times h \times km^2$ to PWh	Explicit conversion factor
Unit conversion for LCOE denominator	$E_T \times 10^{12}$	Converts PWh to kWh in LCOE equations	Explicit conversion factor
Unit conversion for CO_2 reduction	$E_T \times 10^{12}$	Converts PWh to kWh in emission-reduction equations	Explicit conversion factor
Annuity factor γ	Used in wind and PV LCOE equations as the annualized-cost coefficient	Converts investment cost into annualized generation-side cost	The current screening framework does not decompose γ into separate WACC and project-lifetime values
Discount rate/WACC and project lifetime	Not separately parameterized as universal fixed values in the current national-scale screening framework	Related to the annualized-cost term γ	Complete project-finance assumptions would require additional project-level cost data and are identified as a limitation and future research direction

2.9. CO_2 Emission-Reduction Estimation

The CO_2 emission reduction from hydropower generation could be obtained as [61]:

$$ER_{Wa} = \left(EF_{grid} - EF_{Wa}\right) \times E_{T,Wa} \times 10^{12} \quad (10)$$

where ER_{Wa} represents CO_2 emission reduction from hydropower generation, kg CO_2; EF_{grid} denotes the grid emission factor of conventional power generation, kg CO_2/kWh;

EF_{Wa} indicates carbon emission factor of hydropower generation, kg CO_2/kWh; and $E_{T,Wa}$ is technical potential of hydropower generation, PWh.

The CO_2 emission reduction of wind-power generation can be derived as [61]:

$$ER_{Wi} = \left(EF_{grid} - EF_{Wi}\right) \times E_{T,Wi} \times 10^{12} \quad (11)$$

where ER_{Wi} represents CO_2 emission reduction from wind-power generation, kg CO_2; EF_{grid} denotes the grid emission factor of conventional power generation, kg CO_2/kWh; EF_{Wi} is emission factor of wind-power generation, kg CO_2/kWh; and $E_{T,Wi}$ indicates technical potential of wind-power generation, PWh.

The CO_2 emission reduction of PV power generation can be estimated as [61]:

$$ER_{Pv} = \left(EF_{grid} - EF_{Pv}\right) \times E_{T,Pv} \times 10^{12} \quad (12)$$

where ER_{Pv} represents CO_2 emission reduction of PV power generation, kg CO_2; EF_{grid} denotes the grid emission factor of conventional power generation, kg CO_2/kWh; EF_{Pv} denotes the emission factor of PV power generation, kg CO_2/kWh; and $E_{T,Pv}$ corresponds to technical potential of PV power generation, PWh. In Equations (10)–(12), the factor 10^{12} converts technical potential from PWh to kWh.

For example, under the historical scenario, the PV technical potential is 72.6069 PWh and the reported PV-related CO_2 reduction is 79.0581 $\times$ 10^8 t CO_2. This corresponds to an implied net avoided-emission coefficient of 0.1089 kg CO_2/kWh, not 0.1089 g CO_2/kWh.

3. Results

3.1. Hydropower Potentials and CO_2 Emission Reductions

3.1.1. Geographic Potential of Hydropower Generation

The geographical potential of hydropower generation across China's terrestrial river basins is presented in Figure 7. The results demonstrate that the spatial patterns of hydropower potential remain basically consistent with the four representative scenarios (Historical, SSP126, SSP245, and SSP585). Overall, the Yangtze and Pearl River basins exhibit substantially greater geographical potential, while the Haihe, Huaihe, Northern Inland and Xinjiang River basins show relatively limited potential. The Southwestern International Rivers, Yellow River, Northeastern Rivers, and Southeastern Coastal Rivers display intermediate levels of potential. For instance, the geographical potential of the Yangtze River basin is approximately 2 to 2.5 times that of the Pearl River basin, and about 4 to 4.5 times that of the Yellow River basin. Compared to Historical scenario, the Southwestern International Rivers, Pearl River subregion 1, and Yangtze River basin show significant increases in geographical potential under future scenarios, with growth rates reaching 44%, 33%, and 26% respectively. Conversely, the Haihe River, Yellow River, and Southeastern Coastal subregion 1 all demonstrate lower geographical potential in future scenarios compared to Historical scenario.

3.1.2. Technical Potential of Hydropower Generation

The spatial patterns of hydropower technical potential (Figure 8) are generally consistent with those of geographical potential (Figure 7) across different river basins. Furthermore, the changes in technical potential under future scenarios compared to Historical scenario are largely similar to the variations observed in geographical potential. More specifically, the Yangtze River basin, Southwestern International Rivers, and Pearl River subregion 1 show more significant increases in technical potential under future scenarios relative to Historical scenario, while the technical potentials in other river basins remain relatively similar across all four scenarios. The Yangtze River basin exhibits substantially

higher technical potential than other basins, reaching approximately 1.44 PWh under SSP585 scenario (the highest) and about 1.15 PWh under Historical scenario (the lowest). The Pearl River subregion 1 ranks second in technical potential following the Yangtze River basin, while the Southwestern International Rivers rank third. The technical potentials of the Southeastern Coastal Rivers subregion 1, Yellow River basin, and Northeastern Rivers fall into intermediate levels, whereas the Southeastern Coastal Rivers subregion 2 and Pearl River subregion 2 demonstrate the lowest technical potentials.

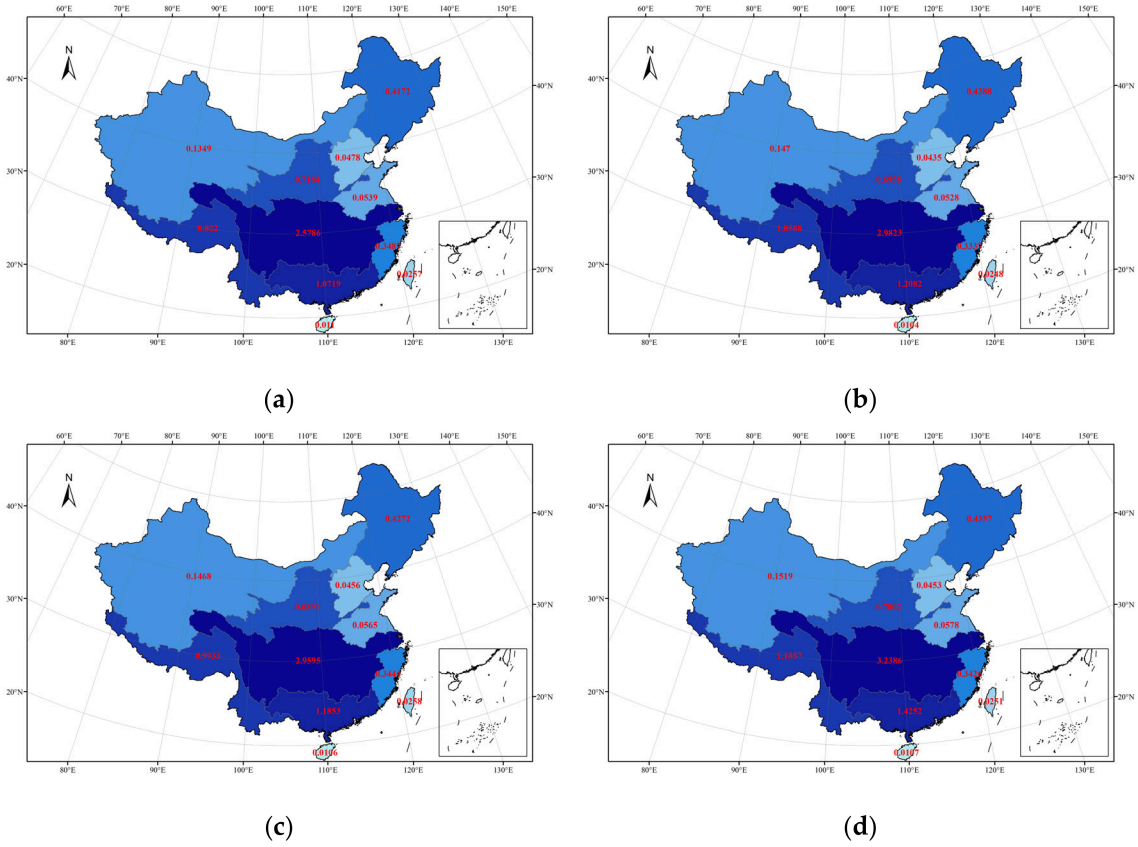


Figure 7. Hydropower geographic potentials under (**a**) Historical, (**b**) SSP126, (**c**) SSP245, and (**d**) SSP585 scenarios (Unit: PWh).

3.1.3. Economic Potential of Hydropower Generation

The cost–supply curves of hydropower generation under four representative scenarios across different river basins are presented in Figure 9. It is demonstrated that the electricity supply quantity (economic potential) generally increases gradually with rising unit production costs. The changing slope of the curves reflects both the cost dependence of supply quantity and the economic feasibility of power production and supply. Consequently, the specific value of economic potential depends on the corresponding unit production cost (i.e., LCOE). For instance, under Historical scenario, the Yangtze River basin demonstrates an economic potential of approximately 1.13 PWh when the levelized cost reaches 0.4 Yuan/kWh. When the cost decreases to 0.2 Yuan/kWh, the corresponding economic potential declines to about 0.05 PWh. Similarly, the economic potential of hydropower generation at specified cost levels in each river basin could be quantitatively determined from the established cost–supply curves through graphical interpolation.

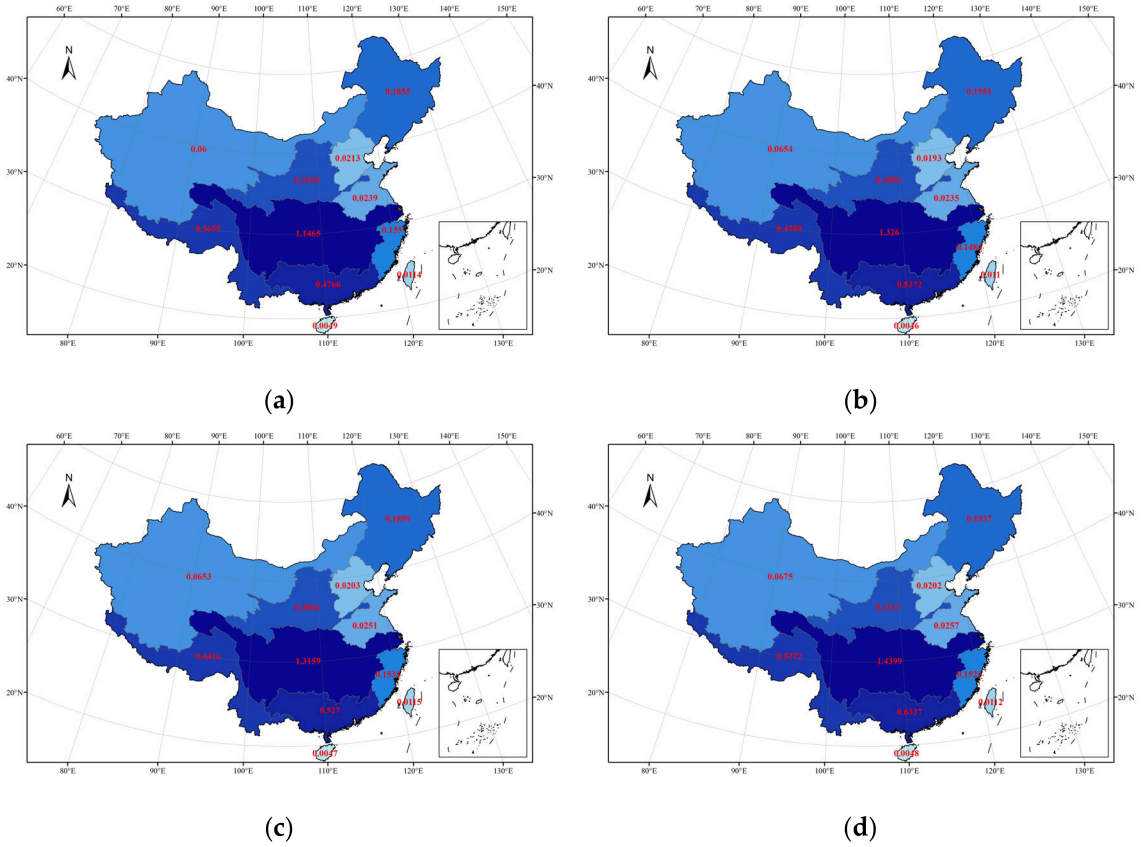


Figure 8. Hydropower technical potentials under (**a**) Historical, (**b**) SSP126, (**c**) SSP245, and (**d**) SSP585 scenarios (Unit: PWh).

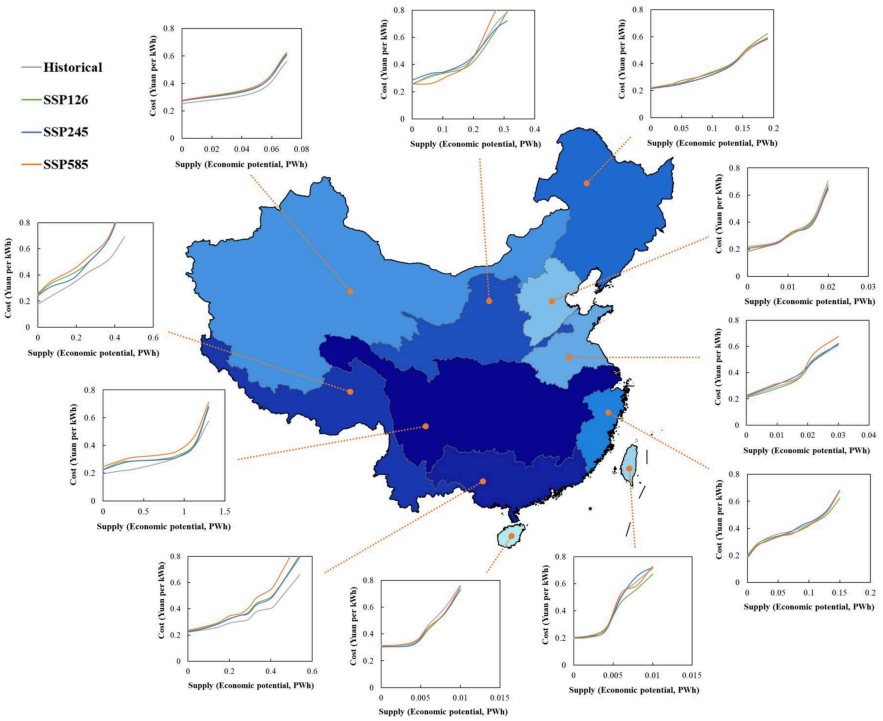


Figure 9. Hydropower cost–supply curves and economic potentials under Historical, SSP126, SSP245, and SSP585 scenarios (Unit: PWh).

The Yangtze River, Pearl River subregion 1, Southwestern International Rivers, Yellow River, and Northeastern Rivers exhibit relatively greater economic potential. At lower cost

levels (e.g., 0.2–0.4 Yuan/kWh), economic potential increases substantially with rising costs. However, when costs continue to increase and reach higher levels (e.g., >0.6 Yuan/kWh), the economic potential no longer shows significant growth. These river basins demonstrate better economic viability for hydropower generation, characterized by lower LCOE and greater economic potential. On the other hand, the cost–supply curves for future scenarios in the Northern Inland and Xinjiang Rivers, Southwestern International Rivers, Yangtze River, and Pearl River subregion 1 all lie above their Historical counterparts. In other words, for any given LCOE, the economic potential under future scenarios would be lower than under Historical scenario.

3.1.4. CO_2 Emission Reduction from Hydropower Generation

Figure 10 displays the CO_2 emission reductions from hydropower generation in different river basins under various scenarios. The results show that future scenarios achieve greater emission reductions than Historical scenario for the Yangtze River, Pearl River subregion 1, Southwestern International Rivers, Northeastern Rivers, and Northern Inland and Xinjiang Rivers. The Yellow River basin demonstrates marginally lower CO_2 emission reductions in future scenarios (4.4×10^7 t CO_2) compared to Historical scenario (4.6×10^7 t CO_2). Meanwhile, other basin regions, including the Haihe River, Huaihe River, Southeastern Coastal Rivers, and Pearl River subregion 2, exhibit negligible variations in emission reductions across different future scenarios relative to Historical baseline.

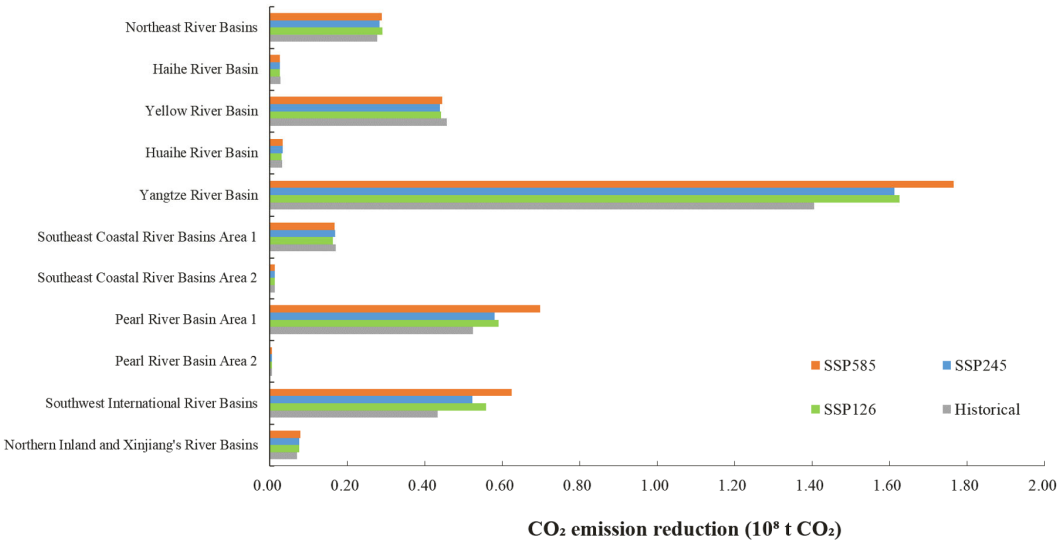


Figure 10. Hydropower CO_2 emission reduction under Historical, SSP126, SSP245, and SSP585 scenarios.

3.2. Wind-Power Potentials and CO_2 Emission Reductions

3.2.1. Geographic Potential of Wind Power Generation

The geographical potential of wind power generation across China's provinces is shown in Figure 11. The results demonstrate that the spatial patterns of wind-power potential under the four representative scenarios (Historical, SSP126, SSP245, and SSP585) remain largely consistent. Overall, Northwestern, Northeastern and Southwestern China exhibit relatively greater geographical potential, while Central-Eastern and Southern regions show comparatively smaller potential. Xinjiang ranks first among all provinces, with Historical and future scenario potentials reaching about 5.6 and 4.9 PWh respectively. Other provinces with significant potential include Inner Mongolia, Qinghai, Xizang, Heilongjiang and Gansu, ranging between 1.2 and 3.2 PWh. Sixteen provinces show higher geographical potential in future scenarios compared to Historical scenario, with Guizhou, Guangdong, Guangxi, Hebei, Xizang and Shanxi exhibiting the most notable increases (22% to 46%).

Conversely, eleven provinces demonstrate reduced potential in future scenarios, with Taiwan, Zhejiang, Hainan, Fujian and Xinjiang showing the most significant decreases (all exceeding 10%).

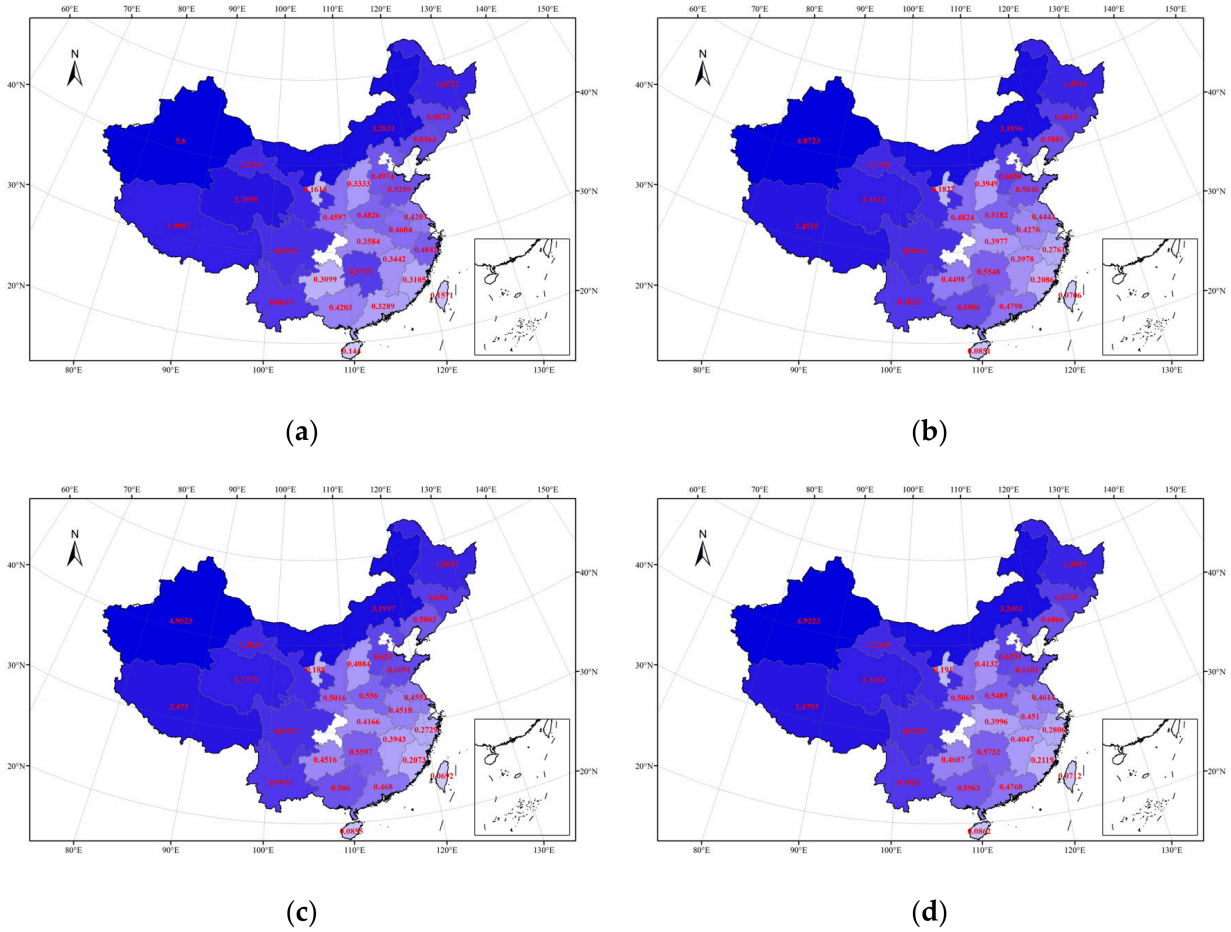


Figure 11. Wind-power geographic potentials under (**a**) Historical, (**b**) SSP126, (**c**) SSP245, and (**d**) SSP585 scenarios (Unit: PWh).

3.2.2. Technical Potential of Wind Power Generation

The spatial patterns of wind-power technical potential (Figure 12 are generally consistent with those of geographical potential (Figure 11). Overall, provinces with greater geographical potential tend to demonstrate higher technical potential. For instance, Xinjiang, Inner Mongolia, Qinghai, Xizang, and Heilongjiang all exhibit technical potentials exceeding 1.1 PWh. Sixteen provinces exhibit higher technical potential under future scenarios compared to Historical scenario. Among them, Guizhou, Guangdong, and Guangxi demonstrate an increase of over 100%, while Hebei, Shanxi, and Xizang show an increase exceeding 40%. The increases in Jiangxi, Hubei, and Jilin surpass 30%, whereas Ningxia, Shandong, and Henan experience growth of more than 20%. In contrast, eleven provinces show lower technical potential under future scenarios than Historical scenario. Notably, Taiwan, Fujian, Zhejiang, and Hainan exhibit the most substantial declines, all exceeding 50%. Xinjiang experiences a reduction of nearly 20%, while Yunnan, Heilongjiang, and Gansu also register decreases of over 10%.

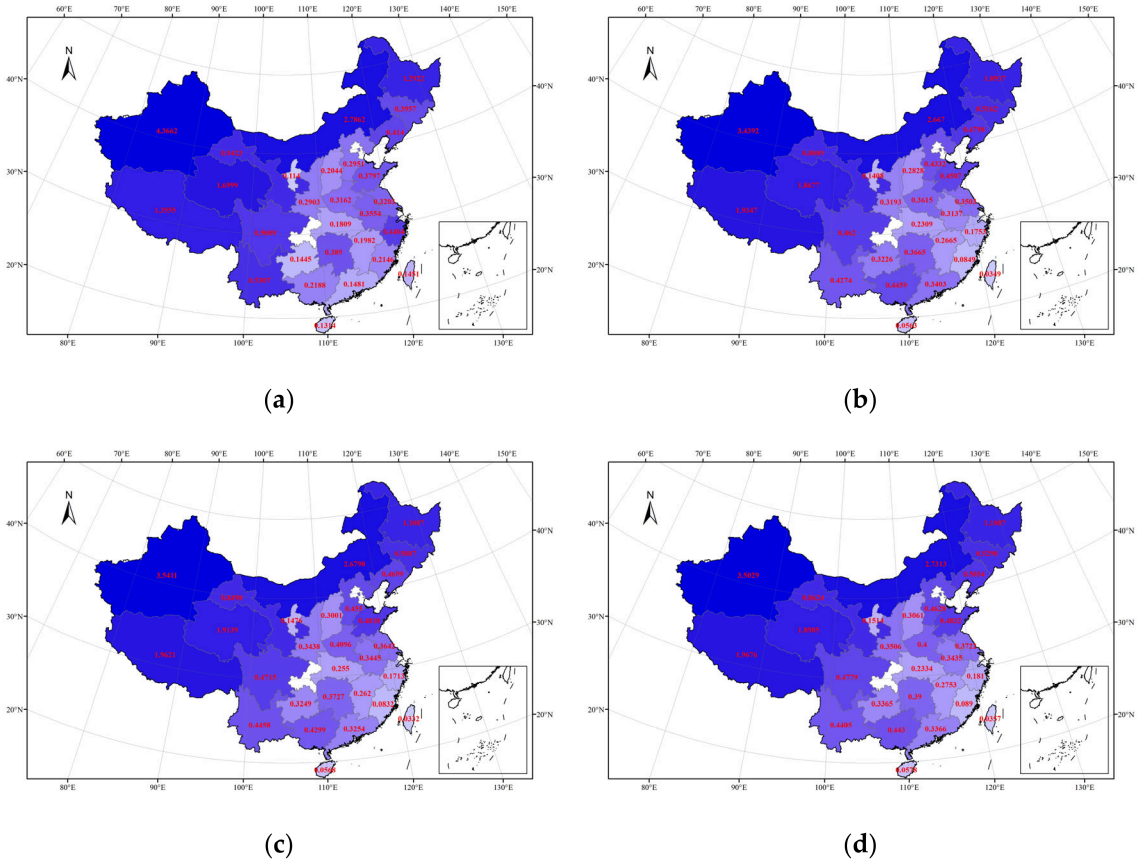


Figure 12. Wind-power technical potentials under (**a**) Historical, (**b**) SSP126, (**c**) SSP245, and (**d**) SSP585 scenarios (Unit: PWh).

3.2.3. Economic Potential of Wind Power Generation

The wind-power cost–supply curves for four typical scenarios are illustrated in Figure 13. The results reveal significant variations in curve patterns among different cost levels, scenarios, and provinces. For more than half of the provinces, the slope of the curve exhibits a transition from gentle to steep. Specifically, at lower cost levels, cost increases exert a pronounced effect on the expansion of economic potential. However, as costs continue to rise and reach higher thresholds, this influence diminishes, and economic potential no longer demonstrates substantial growth. This trend is observed in provinces including Xinjiang, Qinghai, Xizang, Sichuan, Yunnan, Guizhou, Shaanxi, Hunan, Hubei, Guangdong, and Zhejiang. The positions of the cost–supply curves vary across scenarios. If the curve under future scenario lies above that of Historical scenario, the economic potential at a given cost will be lower under future scenarios compared to Historical baseline. This pattern is observed in provinces such as Xinjiang, Gansu, Hunan, Hubei, and Jiangxi. Conversely, if the future scenario curve is positioned below the Historical one, the economic potential at a given cost will be higher under future scenarios, as seen in Xizang, Inner Mongolia, Heilongjiang, Jilin, Hebei, Shandong, Guizhou, Guangxi, and Guangdong. The vertical positions of the curves vary across provinces, reflecting distinct spatial patterns in economic potential and cost-effectiveness. Overall, regions in Northwest (e.g., Xinjiang, Qinghai, Gansu, Inner Mongolia), Southwest (e.g., Xizang, Sichuan, Yunnan), and Northeast China (e.g., Heilongjiang, Jilin) exhibit both high economic potential and superior cost-effectiveness. Certain provinces in North and East-Central China (e.g., Hebei, Henan, Shandong, Hunan) also demonstrate considerable economic potential, though with relatively constrained cost-effectiveness. For instance, at a cost of 0.2 Yuan/kWh, the average economic potential of Xinjiang and Xizang under future scenarios reaches

2.40 and 1.42 PWh, respectively, underscoring their exceptional economic viability and vast exploitable potential.

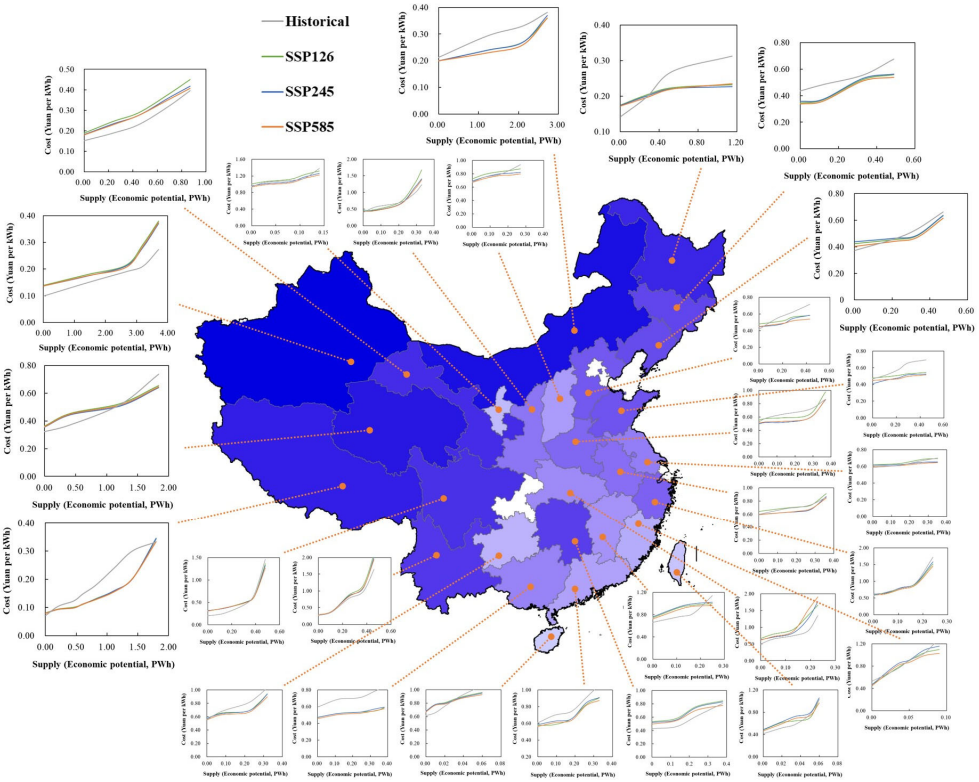


Figure 13. Wind-power cost–supply curves and economic potentials under Historical, SSP126, SSP245, and SSP585 scenarios (Unit: PWh).

3.2.4. CO_2 Emission Reduction from Wind Power Generation

Figure 14 presents the CO_2 emission reductions achieved through wind-power generation under different scenarios. Comparative analysis reveals that sixteen provinces exhibit greater emission reductions under future scenarios compared to Historical scenario. Xizang demonstrates the most substantial increase in absolute terms (approximately 3.8×10^7 t CO_2), representing a 44.3% enhancement. The provinces of Guizhou, Guangdong, and Guangxi all show emission reduction increases exceeding 100%, while other provinces with significant increases include Hebei, Qinghai, Jilin, and Shanxi. In contrast, ten provinces show decreased emission reduction under future scenarios. Xinjiang experiences the most pronounced decline (approximately 5.4×10^7 t CO_2), corresponding to a decrease of 19.9%. Fujian and Hainan exhibit decreases exceeding 50%, with other notable decreases observed in Heilongjiang and Inner Mongolia.

3.3. Photovoltaic-Power Potentials and CO_2 Emission Reductions

3.3.1. Geographic Potential of PV Power Generation

The geographical potential of PV power generation across China's terrestrial areas is presented in Figure 15. As illustrated, the spatial patterns of geographical potential remain largely consistent among the four representative scenarios (Historical, SSP126, SSP245, and SSP585). Overall, Northwestern, Northern, Northeastern, and certain Southeastern regions of China exhibit relatively high geographical potential, while Central and Southwestern regions demonstrate comparatively lower values. Xizang ranks highest among all provinces, with geographical potentials reaching approximately 12.3 PWh under Historical scenario and 13.2 PWh under future scenarios. Provinces following Xizang in geographical potential include Xinjiang, Inner Mongolia, Ningxia, Qinghai, and Gansu, all exceeding 5.0 PWh.

Except for Ningxia, Jiangxi, Zhejiang, Guangdong, and Guangxi under SSP585 scenario, all provinces show higher geographical potential in future scenarios compared to Historical scenario. The most notable increases in geographical potential under future scenarios are observed in Yunnan, Liaoning, Shandong, Jilin, and Sichuan, where the growth exceeds 0.5 PWh, representing an increase of more than 20%.

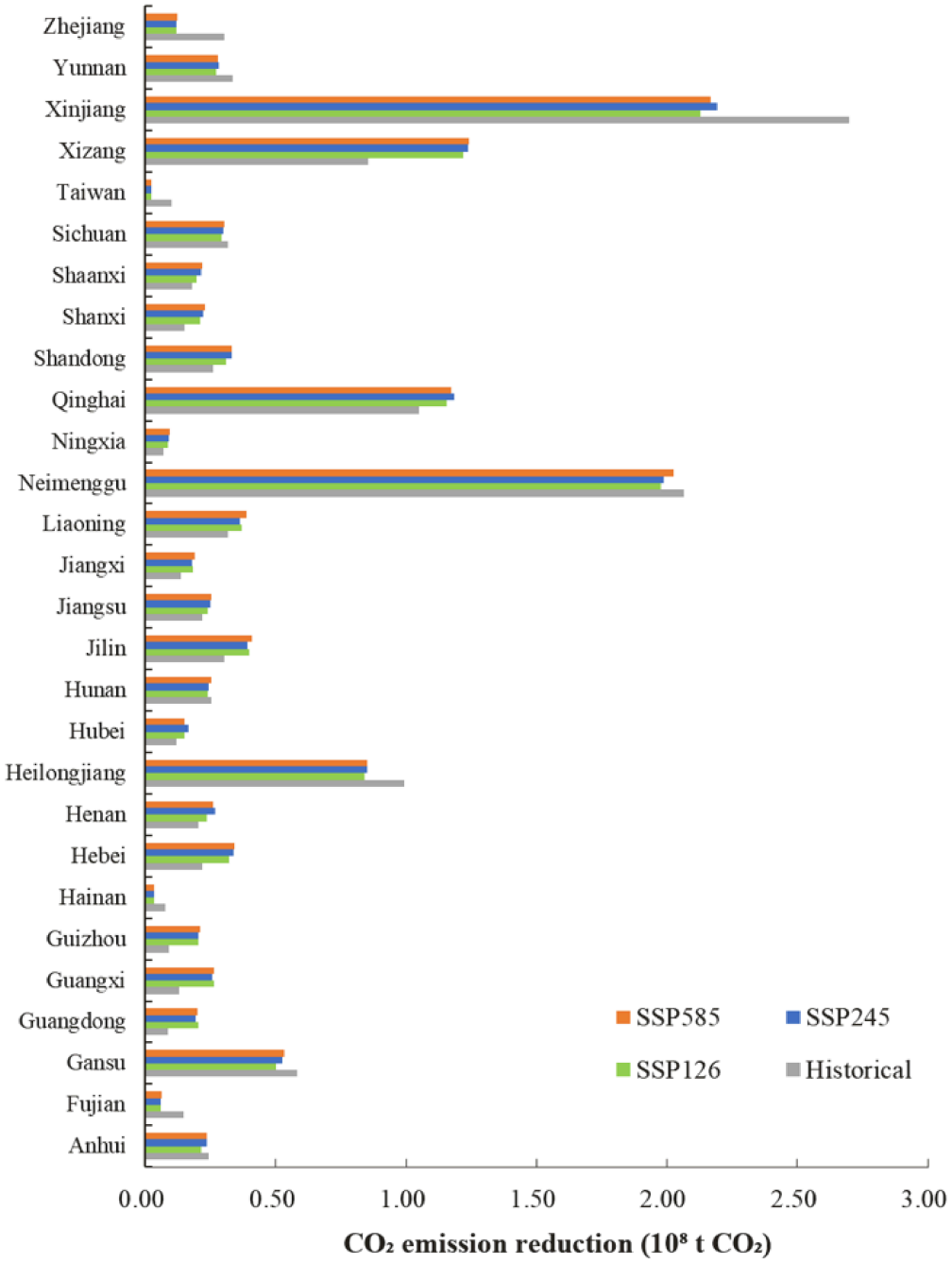


Figure 14. Wind-power CO_2 emission reduction under Historical, SSP126, SSP245, and SSP585 scenarios.

3.3.2. Technical Potential of PV Power Generation

The spatial patterns of provincial technical potential (Figure 16) and geographical potential (Figure 15) for PV power generation are basically consistent. Generally, regions with higher geographical potential also exhibit greater technical potential. For instance, provinces such as Xizang, Xinjiang, Inner Mongolia, Ningxia, Qinghai, and Gansu all have technical potentials exceeding 3.0 PWh. Moreover, the changes in technical potential

under future scenarios compared to Historical scenario align closely with those observed in geographical potential. Provinces such as Yunnan, Liaoning, Shandong, Jilin, and Sichuan show an increase in technical potential of over 0.3 PWh in future scenarios relative to Historical scenario. Additionally, Xizang and Xinjiang exhibit significant growth, with increases of 0.58 and 0.39 PWh, respectively, in their future-scenario technical potentials.

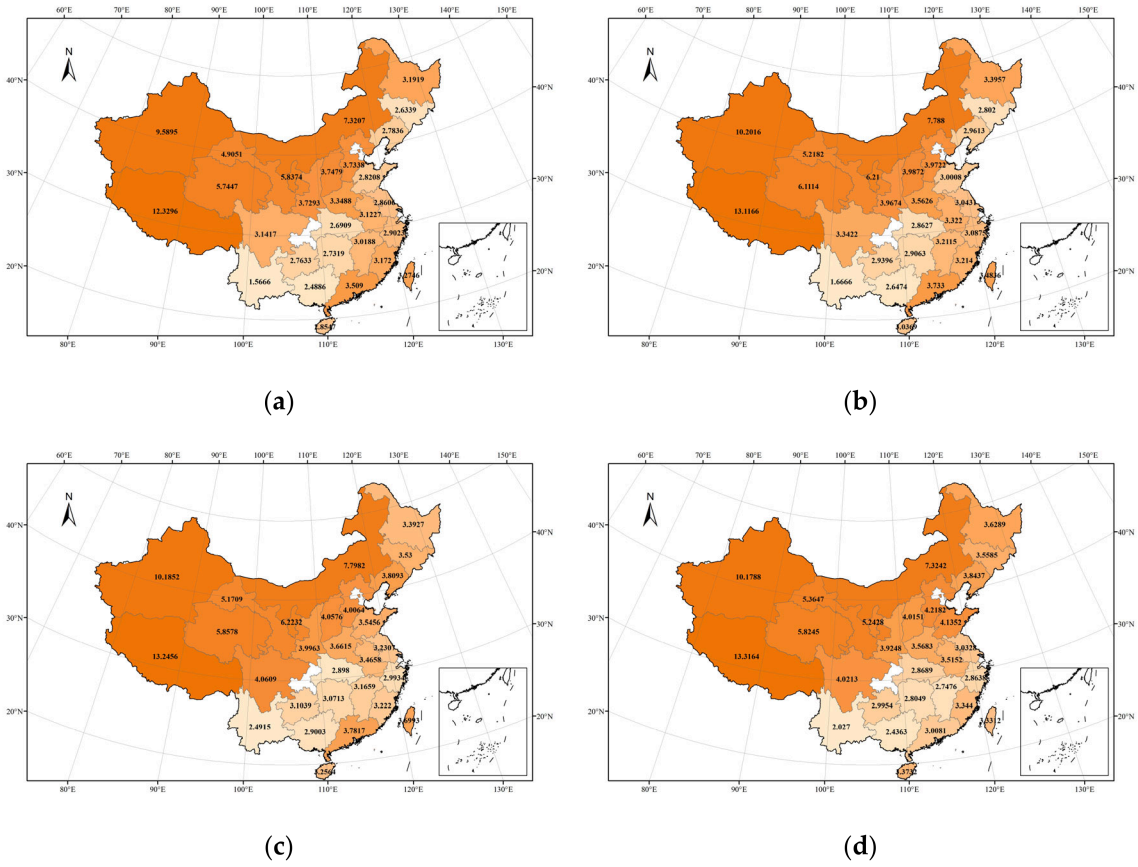


Figure 15. Photovoltaic-power geographic potentials under (**a**) Historical, (**b**) SSP126, (**c**) SSP245, and (**d**) SSP585 scenarios (Unit: PWh).

3.3.3. Economic Potential of PV Power Generation

The PV power generation cost–supply curves under four representative scenarios for each province are presented in Figure 17. The results indicate that electricity supply (economic potential) generally increases with rising LCOE, though variations exist in curve shapes across different cost ranges, scenarios, and provinces. For instance, provinces such as Shanxi, Shaanxi, Hebei, Jiangsu, and Qinghai exhibit gentler-sloped, nearly linear curves, suggesting a gradual increase in economic potential with higher costs. In contrast, most other provinces display steeper curves, indicating a more rapid expansion of economic potential as costs rise. This trend is particularly pronounced in Xinjiang, Xizang, Yunnan, Gansu, and Ningxia, where the economic potential grows substantially with marginal cost increases. The positioning of provincial cost–supply curves varies across different scenarios. For most provinces, future scenario curves fluctuate near Historical scenario curve, indicating that their economic potentials under future scenarios will generally remain comparable to Historical baseline. However, provinces including Qinghai, Guangxi, Hainan, Hunan, Hubei, Jiangxi, Jiangsu, and Liaoning exhibit future scenario curves positioned above Historical curve. This upward shift suggests that their economic potentials under future scenarios will be lower than those under Historical scenario. The vertical positioning of the curves varies across provinces, reflecting spatial disparities in economic

potential and cost-effectiveness. Overall, China's Northwestern (Xinjiang, Inner Mongolia, Ningxia, Qinghai, Gansu), Southwestern (Xizang, Yunnan, Sichuan), and Northeastern regions (Heilongjiang, Jilin) demonstrate both substantial economic potential and superior cost-effectiveness. Northern China and certain coastal areas in the Southeast (Shanxi, Hebei, Henan, Shandong, Anhui, Zhejiang, Fujian, Guangdong) also possess considerable economic potential, though with relatively constrained cost-effectiveness. For instance, at a LCOE of 0.2 Yuan/kWh, Xizang exhibits economic potentials of 0.5 PWh (Historical scenario) and 1.05 PWh (SSP126 scenario), underscoring its exceptional economic potential and favorable cost-efficiency.

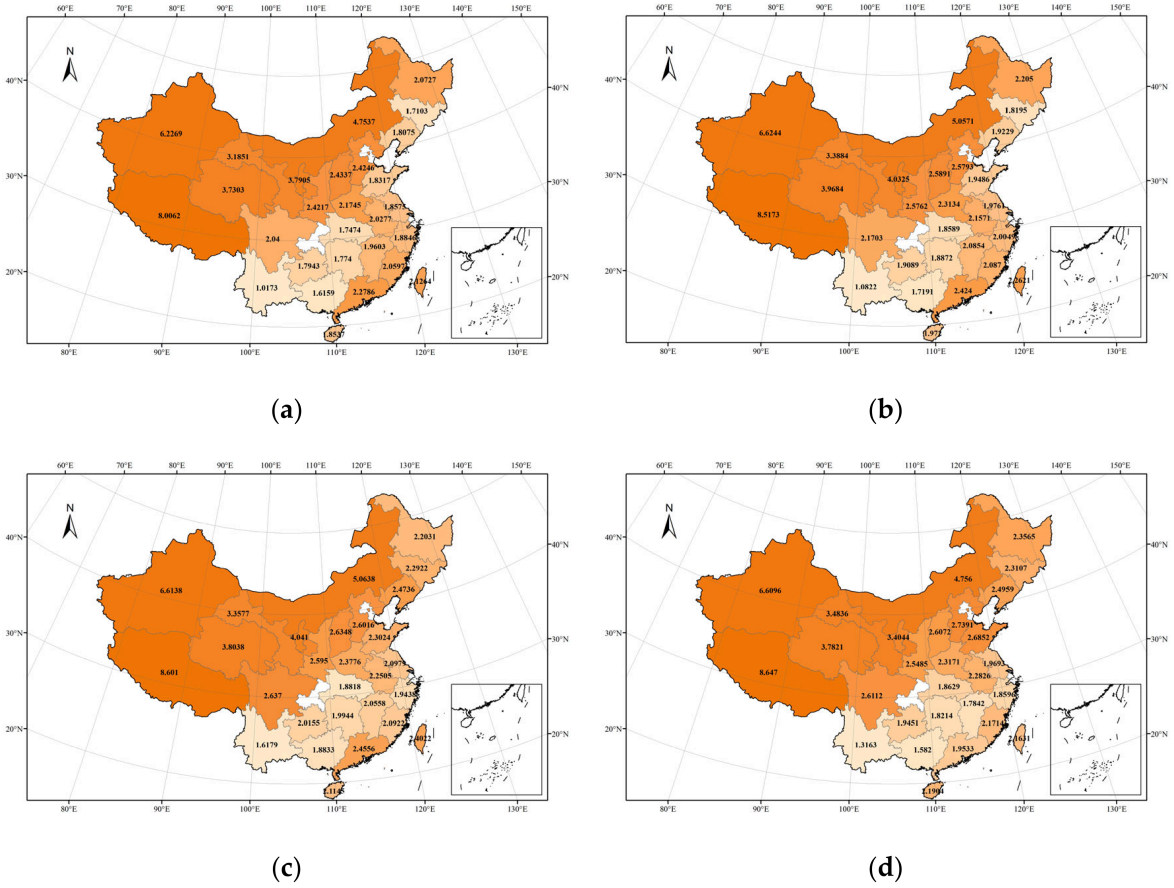


Figure 16. Photovoltaic-power technical potentials under (**a**) Historical, (**b**) SSP126, (**c**) SSP245, and (**d**) SSP585 scenarios (Unit: PWh).

3.3.4. CO_2 Emission Reduction from PV Power Generation

Figure 18 presents provincial CO_2 emission reductions from PV power generation under different scenarios. Twenty-three provinces demonstrate greater emission reductions in all three future scenarios compared to Historical scenario. Xizang exhibits both the highest absolute emission reductions and the largest incremental increase (approximately 6.1×10^8 t CO_2) between Historical and future scenarios. Notable increases in emission reductions are also observed in Liaoning, Shandong, Jilin, Sichuan, Xinjiang, and Yunnan, with increments ranging between 3.4×10^8 and 5.9×10^8 t CO_2 under future scenarios. Conversely, five provinces (Ningxia, Jiangxi, Zhejiang, Guangdong, and Guangxi) show lower emission reductions under SSP585 scenario compared to Historical scenario.

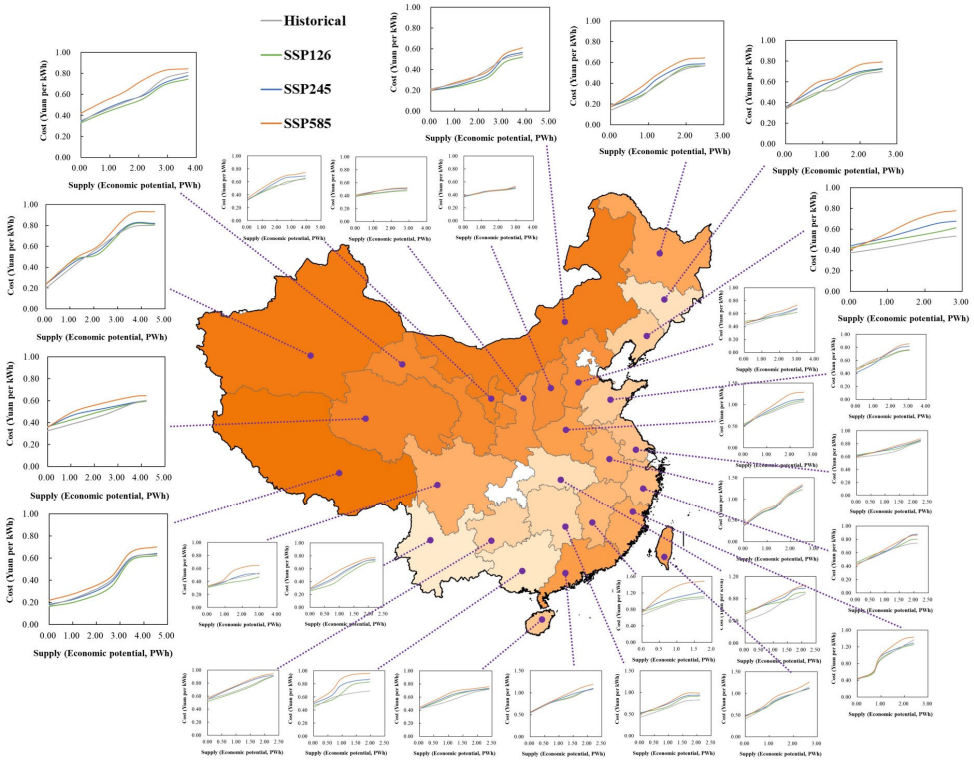


Figure 17. Photovoltaic-power cost–supply curves and economic potentials under Historical, SSP126, SSP245, and SSP585 scenarios (Unit: PWh).

3.4. Total Results of Terrestrial China

In total, the energy utilization potentials and CO_2 emission reductions of China's terrestrial areas are comprehensively quantified (Table 6), based on the model calculation parameters presented (Table 7). The results indicate that under Historical scenario, hydropower demonstrates geographical potential, technical potential, and emission reductions of approximately 6.23 PWh, 2.77 PWh, and 3.41 $\times$ 10^8 t CO_2, respectively. For three future scenarios, the average values increase to approximately 7.17 PWh (geographical potential), 3.19 PWh (technical potential), and 3.91 $\times$ 10^8 t CO_2 (emission reductions). This represents an approximate 15% enhancement in power generation potential and a 14.5% increase in emission reduction capacity compared to Historical scenario. Under Historical scenario, wind power demonstrates geographical potential, technical potential, and CO_2 emission reductions of approximately 25.70 PWh, 18.77 PWh, and 12.50 $\times$ 10^8 t CO_2, respectively. The average values of three future scenarios show modest increases to approximately 25.90 PWh (geographical potential), 19.02 PWh (technical potential), and 12.67 $\times$ 10^8 t CO_2 (emission reductions). These represent marginal growth rates of 0.78%, 1.33%, and 1.32%, respectively, compared to Historical baseline. Under Historical scenario, PV power generation demonstrates geographical potential, technical potential, and CO_2 emission reductions of approximately 111.81 PWh, 72.61 PWh, and 79.06 $\times$ 10^8 t CO_2, respectively. The average values of three future scenarios show increases to approximately 121.04 PWh (geographical potential), 78.60 PWh (technical potential), and 85.67 $\times$ 10^8 t CO_2 (emission reductions). This represents an 8.3% enhancement in power generation potential and an 8.4% increase in emission reduction capacity compared to Historical scenario.

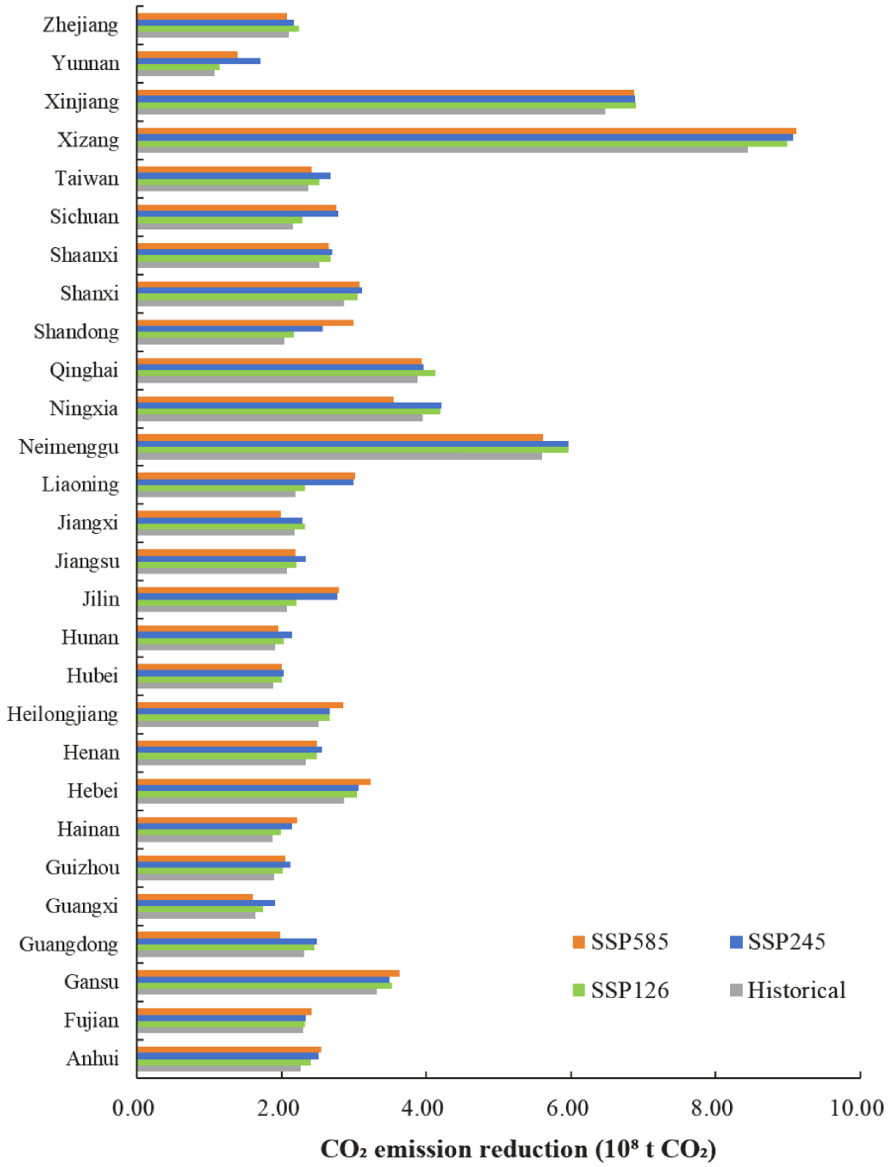


Figure 18. Photovoltaic-power CO_2 emission reduction under Historical, SSP126, SSP245, and SSP585 scenarios.

Table 6. China's terrestrial hydro-, wind-, and photovoltaic-power potentials and CO_2 emission reductions.

Renewable Power Type	Potential or Emission Reduction	Four Selected Scenarios			
		Historical	SSP126	SSP245	SSP585
Hydro-power energy	Geographic potential (PWh)	6.2300	6.9961	6.8842	7.6188
	Technical potential (PWh)	2.7700	3.1106	3.0609	3.3875
	CO_2 emission reduction (10^8 t CO_2)	3.4132	3.8196	3.7587	4.1441
Wind-power energy	Geographic potential (PWh)	25.7001	25.6240	25.9690	26.0935
	Technical potential (PWh)	18.7700	18.6731	19.1124	19.2710
	CO_2 emission reduction (10^8 t CO_2)	12.5046	12.4400	12.7260	12.8420
Photovoltaic-power energy	Geographic potential (PWh)	111.8146	118.7913	123.8215	120.5139
	Technical potential (PWh)	72.6069	77.1372	80.4036	78.2558
	CO_2 emission reduction (10^8 t CO_2)	79.0581	83.9883	87.6302	85.3909

Table 7. Parameter-influence table.

Parameter or Assumption	Direction of Influence on Results
Higher ecological-flow release	Decreases hydropower technical potential
Shorter hydropower site interval	May increase simulated site number and potential, but may overestimate feasible development
Higher wind-power density	Increases wind technical potential nearly proportionally
Higher PV performance ratio	Increases PV technical potential nearly proportionally
Updated land-cover data	May increase or decrease PV suitable area depending on urbanization, ecological protection, and land conversion
Lower future grid emission factor	Decreases estimated future CO_2 emission reductions
Inclusion of storage, curtailment, and transmission costs	Increases system-level cost and reduces practically deployable economic potential

From an absolute value perspective, the three types of energy utilization potential and emission reduction scales follow this order: hydropower < wind power < PV power. Under Historical scenario, wind power demonstrates geographical potential, technical potential, and emission reductions approximately 4.1, 6.8, and 3.7 times greater than those of hydropower, respectively. These ratios become 3.6, 6.0, and 3.2 times under the average future scenarios. More strikingly, PV power under Historical scenario shows geographical potential, technical potential, and emission reductions about 17.9, 26.2, and 23.2 times those of hydropower, respectively. These multiples remain substantial under future scenarios, averaging 16.9, 24.7, and 21.9 times. Similarly, PV power's Historical scenario values are approximately 4.4 times (geographical potential), 3.9 times (technical potential), and 6.3 times (emission reductions) those of wind power, with future scenario averages increasing to 4.7, 4.1, and 6.8 times, respectively. In summary, under the adopted assumptions and screening criteria, PV power shows the largest estimated resource and technical potential, followed by wind power and hydropower. However, this ranking reflects resource-screening results and should not be interpreted as a direct ranking of practical deployability or overall technological superiority.

The results should be interpreted with attention to scenario-level uncertainty. Based on the three future SSP scenarios, hydropower geographic potential ranges from 6.88 to 7.62 PWh, indicating that hydropower is sensitive to changes in runoff and precipitation regimes. Wind-power geographic potential shows a narrower future-scenario range around the historical baseline, suggesting relatively smaller scenario-level variation at the national scale under the adopted assumptions. PV geographic potential ranges from approximately 120.51 to 122.12 PWh across future scenarios, reflecting the influence of solar irradiance and land-suitability assumptions. These ranges provide a first-order indication of scenario-level variability, but they should not be interpreted as full probabilistic confidence intervals. A complete uncertainty analysis would require retaining model-specific CMIP6 outputs, parameter ensembles, and detailed sensitivity tests for hydrological, wind-energy, PV-conversion, economic, and grid-emission assumptions.

The reported potentials should be interpreted as resource-screening estimates rather than immediately deployable capacity. The technical potentials, especially for PV and wind power, indicate substantial resource availability under the adopted land-use, technical, and scenario assumptions. However, only part of this potential can be converted into practical deployment because large-scale development is constrained by land-use planning, ecological protection, grid connection, long-distance transmission, energy storage, curtailment management, investment feasibility, and regional demand matching. For example, northwestern and plateau regions show high wind and PV resource potential, but they are relatively far from major demand centers and may require expanded transmission capacity

and storage support. In eastern and central China, resource potential may be lower, but proximity to load centers may improve demand matching and reduce transmission requirements. Therefore, the ranking of resource potential should not be interpreted as a direct ranking of deployment priority or overall technological superiority.

4. Discussion

4.1. Developed Versus the Remaining Energy Potentials

When assessing future hydropower potential, it should also consider basin-specific factors, including existing power station infrastructure, installed capacity, and annual power generation, i.e., essentially comparing developed versus remaining potential. For instance, river basins in Northeast China currently have relatively few hydropower stations with numerous viable sites available for development, indicating substantial remaining hydropower potential. Based on current statistical data and our estimation results, this region exhibits a future remaining potential to the existing generation ratio of approximately 4:1. Conversely, the Yangtze River basin already hosts multiple large-scale hydropower projects with high total installed capacity and development intensity, resulting in a lower remaining potential ratio of about 3:2.

Similarly, our estimates of future wind and PV power potential also incorporate currently utilized portions. However, the construction and development pace of wind and PV facilities in China is remarkably rapid, with their capacity expansion rates significantly outpacing hydropower. Furthermore, due to limitations in data availability and challenges in obtaining real-time statistics, it remains difficult to accurately quantify the proportional relationship between currently developed versus remaining future potential for wind and PV power generation.

4.2. Analysis on Different Scenarios and Relevant Research

China's terrestrial hydropower potential exhibits notable scenario-dependent variations. Taking geographical potential as an example, the SSP585 scenario yields the highest estimate (7.62 PWh), while SSP245 shows the lowest (6.88 PWh), both exceeding Historical scenario (6.23 PWh). These results align substantially with the estimation of China's annual hydropower potential at approximately 6 PWh by Li et al. (2018) [66]. Hydropower potential demonstrates sensitivity to both climate change and socioeconomic development pathways. The SSP585 scenario, characterized by more pronounced climate change and extreme conditions, may enhance precipitation patterns and water resource availability, thereby increasing generation potential. Conversely, the relatively moderate climate change under SSP126 could somewhat constrain water resources and subsequent power generation capacity. From a socioeconomic perspective, the high-carbon emission and resource-intensive development trajectory of SSP585 scenario not only escalates hydropower demand and development intensity but also elevates its generation potential. In contrast, the more sustainable economic growth pathway of SSP126 may moderately suppress electricity demand, consequently reducing hydropower potential.

Under Historical scenario, China's terrestrial wind-power generation demonstrates geographical and technical potentials of 25.7 and 18.77 PWh, respectively. These values show minor variations across different SSP scenarios while remaining generally comparable to Historical baseline. These estimates appear slightly lower than the estimation of approximately 22.5 PWh of China's wind-power technical potential by Davidson et al. (2016) [45]. This discrepancy might be caused by differences in foundational datasets and methodologies, as well as the exclusion of offshore wind energy resources in the current assessment.

Under Historical scenario, China's terrestrial PV power generation demonstrates a geographical potential of 111.81 PWh, which increases to 120.51 PWh under SSP585 scenario. These estimates are comparatively lower than those in previous studies by Yang et al. (2019) [59] and Qiu et al. (2022) [67], which reported China's PV potential at approximately 138.87 and 131.94 PWh, respectively. These discrepancies may arise from several aspects: (1) differences in data sources, spatial geographic information, and climate models, particularly regarding solar resource and topographic considerations; (2) differing assumptions about technological advancements in PV systems, including projected improvements in module efficiency and cost reductions; and (3) divergent socioeconomic scenario assumptions that influence future energy demands and environmental policies.

4.3. Policy Implications

The results suggest that renewable-energy planning in China should be differentiated by energy type and region rather than based only on the absolute magnitude of estimated resource potential. For hydropower, future development should prioritize ecological-flow protection, river-basin coordination, and careful assessment of remaining developable potential. In basins with high existing hydropower development intensity, such as the Yangtze River basin, further expansion should be evaluated cautiously because additional development may face stronger ecological, social, and engineering constraints. In basins with relatively larger remaining potential, hydropower planning should still account for ecological-flow requirements, downstream water use, sediment transport, and basin-scale conservation objectives.

For wind power, high-potential northern and western provinces should not be interpreted as automatically suitable for immediate large-scale deployment. Wind-power development should be coordinated with grid-integration capacity, transmission corridors, curtailment risk, and regional demand distribution. Provinces with strong wind resources but weak local demand or limited transmission capacity may require additional grid expansion and storage support before their technical potential can be converted into practical generation. Future planning should also incorporate refined hub-height wind-resource assessment, turbine power curves, and site-specific wind-speed distributions to improve project-level deployment decisions.

For PV power, the large estimated potential indicates abundant solar-resource availability under the adopted land-use and technical assumptions, but deployment should be coordinated with land-use planning, ecological protection, grid absorption, and storage requirements. Large-scale PV bases in northwestern and plateau regions can contribute substantially to renewable-energy supply, but they may require long-distance transmission and storage to match demand centers. In eastern and central China, distributed PV deployment near load centers may help reduce transmission pressure and improve demand matching, even though the estimated resource potential is lower than that in western regions. Therefore, PV planning should balance centralized resource-based development with distributed deployment, land availability, ecological constraints, and system-integration costs.

Overall, the policy value of this study lies in identifying relative resource endowments and regional priorities under consistent screening assumptions. The estimated potentials should be used as a first step for strategic planning, while final deployment decisions should integrate ecological protection, land-use regulation, grid expansion, storage, curtailment management, investment feasibility, and regional electricity demand.

4.4. Limitations and Future Research

First, the assessment relies on several spatial and technical assumptions that are necessary for national-scale screening. These include the 30 km hydropower site interval, 30%

ecological-flow release, river-mouth exclusion, wind-power density, and PV performance ratio. These assumptions make the three energy types comparable across China, but they cannot represent all local engineering, ecological, or operational conditions. Future research should conduct parameter sensitivity tests and project-level validation in representative basins and provinces.

Second, land-use and infrastructure constraints are represented in a simplified and static manner. The PV suitability analysis uses GlobCover 2009 and nature-reserve constraints to provide a nationally consistent land-cover baseline. However, recent urban expansion, renewable-energy infrastructure development, ecological-redline policies, local land-use planning, grid proximity, and future land-use change are not dynamically represented. Future studies should incorporate updated high-resolution land-cover products, dynamic land-use scenarios, grid-distance metrics, and regional land-planning constraints.

Third, the economic-potential assessment is based on simplified generation-side LCOE estimates and is intended for national-scale screening rather than project-level techno-economic evaluation. This approach is useful for constructing comparable cost-supply curves across energy types, regions, and scenarios, but it does not represent complete system costs. Although Table 4 improves transparency by distinguishing fixed numerical assumptions from site- or province-specific input cost terms, the current study does not yet provide the complete site-level or province-level cost database that would be required for fully reproducing each cost–supply curve. In addition, storage requirements, curtailment risk, long-distance transmission investment, detailed grid-connection reinforcement, financing heterogeneity, and local electricity-market conditions are not explicitly included. Therefore, the economic-potential results should be interpreted as simplified generation-side screening estimates rather than fully reproducible project-level LCOE or complete system-cost estimates. Future research should develop open project-level cost databases and couple renewable-resource assessment with power-system planning models to incorporate storage, curtailment, transmission expansion, grid-connection costs, financing conditions, and regional market constraints.

Fourth, uncertainty and CO_2 mitigation estimates remain subject to scenario and methodological limitations. Although this study compares historical and SSP-based future scenarios, the reported results do not constitute full probabilistic uncertainty intervals. In addition, CO_2 emission reductions are estimated using static grid emission factors, whereas China's power system is expected to continue decarbonizing. Future research should retain model-specific CMIP6 outputs for ensemble uncertainty analysis, incorporate parameter sensitivity tests, and use dynamic grid-emission factors to evaluate avoided emissions under different power-system transition pathways.

5. Conclusions

This study provides a national-scale comparison of terrestrial hydropower, wind power, and PV power potentials and associated CO_2 emission reductions in China under historical and future SSP scenarios. The main conclusions are as follows:

(1) Hydropower potential is spatially concentrated in the Yangtze River basin, Pearl River basin, and Southwestern International Rivers, reflecting the combined influence of runoff, topography, and river-network conditions. Future scenarios generally show higher hydropower potential than the historical baseline under the adopted assumptions.

(2) Wind-power potential is relatively high in northwestern, northeastern, and plateau regions. However, practical deployment in these regions depends not only on resource availability but also on grid integration, transmission capacity, curtailment management, and proximity to electricity demand.

(3) PV power shows the largest resource and technical potential among the three energy sources under the adopted assumptions, especially in northwestern, northern, northeastern, and selected southeastern regions. This result should be interpreted as a resource-potential ranking rather than evidence that PV is universally superior in practical deployment.

(4) The estimated CO_2 mitigation potential indicates that renewable-energy expansion can contribute substantially to low-carbon power-system transition. However, future avoided emissions may decline as China's power grid decarbonizes, and static emission factors may overestimate long-term mitigation benefits.

(5) Future renewable-energy planning should integrate resource assessment with ecological protection, dynamic land-use change, storage and transmission planning, curtailment management, system-level cost analysis, and dynamic emission-factor scenarios. Such integration is essential for translating large resource potentials into feasible and sustainable deployment pathways.

Author Contributions: Conceptualization, C.Z. and B.L.; methodology, M.M.; software, B.L. and M.M.; validation, B.L. and L.Z., C.Z. and M.M.; formal analysis, C.H.; investigation, B.L. and L.Z.; resources, C.H.; data curation, B.L.; writing—original draft preparation, B.L.; writing—review and editing, B.L.; supervision, B.L.; project administration, C.Z.; funding acquisition, C.Z. All authors have read and agreed to the published version of the manuscript.

Funding: This research was funded by Central Public-interest Scientific Institution Basal Research Fund (Grant number: HKY-JBYW-2024-11 and HKY-JBYW-2025-17), and National Key Research Priorities Program of China (Grant number: 2023YFC3209303 and 2023YFC3209305).

Data Availability Statement: The original contributions presented in this study are included in the article. Further inquiries can be directed to the corresponding author.

Acknowledgments: We would like to thank potential reviewers very much for their valuable comments and suggestions. We also thank my other colleagues' valuable comments and suggestions that have helped improve the manuscript.

Conflicts of Interest: The authors declare no conflict of interest.

References

1. Jorgenson, A.K.; Alekseyko, A.; Giedraitis, V. Energy Consumption, Human Well-Being and Economic Development in Central and Eastern European Nations: A Cautionary Tale of Sustainability. *Energy Policy* **2014**, *66*, 419–427. [CrossRef]
2. Pérez-Denicia, E.; Fernández-Luqueño, F.; Vilariño-Ayala, D.; Montaño-Zetina, L.; Maldonado-López, L. Renewable Energy Sources for Electricity Generation in Mexico: A Review. *Renew. Sustain. Energy Rev.* **2017**, *78*, 597–613. [CrossRef]
3. Florescu, A.-M.S.; Bandoc, G.; Degeratu, M. Applying Energy Correction Coefficients in Wind Energy Assessment. *Energy Procedia* **2017**, *112*, 579–584. [CrossRef]
4. IEA. *World Energy Outlook*; OECD/IEA: Paris, France, 2009.
5. Logesh, R. Resources, Configurations, and Soft Computing Techniques for Power Management and Control of Pv/Wind Hybrid System. *Renew. Sustain. Energy Rev.* **2017**, *69*, 129–143. [CrossRef]
6. Gerland, P.; Raftery, A.E.; Ševčíková, H.; Li, N.; Gu, D.; Spoorenberg, T.; Alkema, L.; Fosdick, B.; Chunn, J.; Lalic, N.; et al. World Population Stabilization Unlikely This Century. *Science* **2014**, *346*, 234–237. [CrossRef] [PubMed]
7. Allen, S.K.; Plattner, G.-K.; Nauels, A.; Tignor, M.; Xia, Y.; Bex, V.; Midgley, P.; Qin, D.; Stocker, T. Climate Change 2013: The Physical Science Basis. In *An Overview of the Working Group 1 Contribution to the Fifth Assessment Report of the Intergovernmental Panel on Climate Change (IPCC)*; Cambridge University Press: Cambridge, UK, 2014; p. 3544.
8. Pachauri, R.K.; Allen, M.R.; Barros, V.R.; Broome, J.; Cramer, W.; Christ, R.; Church, J.A.; Clarke, L.; Qin, D.; Dasgupta, P.; et al. Climate Change 2014: Synthesis Report. In *Contribution of Working Groups I, II and III to the Fifth Assessment Report of the Intergovernmental Panel on Climate Change*; IPCC: Geneva, Switzerland, 2014.
9. Sağlam, Ü. A Two-Stage Data Envelopment Analysis Model for Efficiency Assessments of 39 State's Wind Power in the United States. *Energy Convers. Manag.* **2017**, *146*, 52–67.

10. Mcglade, C.; Ekins, P. The Geographical Distribution of Fossil Fuels Unused When Limiting Global Warming to 2 °C. *Nature* **2015**, *517*, 187–190. [CrossRef] [PubMed]
11. Fawcett, A.A.; Iyer, G.C.; Clarke, L.E.; Edmonds, J.A.; Hultman, N.E.; Mcjeon, H.C.; Rogelj, J.; Schuler, R.; Alsalam, J.; Asrar, G.R.; et al. Can Paris Pledges Avert Severe Climate Change? *Science* **2015**, *350*, 1168–1169. [CrossRef] [PubMed]
12. Rockström, J.; Gaffney, O.; Rogelj, J.; Meinshausen, M.; Nakicenovic, N.; Schellnhuber, H.J. A Roadmap for Rapid Decarbonization. *Science* **2017**, *355*, 1269–1271. [CrossRef] [PubMed]
13. Bataille, C.; Waisman, H.; Colombier, M.; Segafredo, L.; Williams, J. The Deep Decarbonization Pathways Project (DDPP): Insights and Emerging Issues. *Clim. Policy* **2016**, *16*, S1–S6. [CrossRef]
14. Bataille, C.; Waisman, H.; Colombier, M.; Segafredo, L.; Williams, J. The Need for National Deep Decarbonization Pathways for Effective Climate Policy. *Clim. Policy* **2016**, *16*, S7–S26. [CrossRef]
15. Pye, S.; Bataille, C. Improving Deep Decarbonization Modelling Capacity for Developed and Developing Country Contexts. *Clim. Policy* **2016**, *16*, S27–S46. [CrossRef]
16. Usubiaga, A.; Acosta-Fernández, J.; Mcdowall, W.; Li, F.G.N. Exploring the Macro-Scale CO2 Mitigation Potential of Photovoltaics and Wind Energy in Europe's Energy Transition. *Energy Policy* **2017**, *104*, 203–213.
17. DDPP (Deep Decarbonization Pathways Project). *Pathways to Deep Decarbonization-2014 Report*; Institute for Sustainable Development and International Relations (IDDRI) & Sustainable Development Solutions Network (SDSN): Paris, France, 2014.
18. Florescu, A.M.S.; Bandoc, G.; Degeratu, M. Energy Efficiency Evaluation of Wind Energy Based on Energy Reports. *Adv. Mater. Res.* **2014**, *1008*, 188–191. [CrossRef]
19. Bandoc, G.; Florescu, A.-M.S.; Degeratu, M.; Pravalie, R. Use of Hybrid Renewable Energy Systems for Small Communities. *Renew. Energy Environ. Sustain.* **2016**, *1*, 29. [CrossRef]
20. De Jong, P.; Dargaville, R.; Silver, J.; Utembe, S.R.; Kiperstok, A.; Torres, E.A. Forecasting High Proportions of Wind Energy Supplying the Brazilian Northeast Electricity Grid. *Appl. Energy* **2017**, *195*, 538–555. [CrossRef]
21. Becerra, M.; Moran, J.; Jerez, A.; Cepeda, F.; Valenzuela, M. Wind Energy Potential in Chile: Assessment of a Small Scale Wind Farm for Residential Clients. *Energy Convers. Manag.* **2017**, *140*, 71–90. [CrossRef]
22. CEER. *Position on the European Commission's Policy Framework for Climate and Energy 2020–2030*; CEER: Brussels, Belgium, 2014.
23. Proietti, S.; Sdringola, P.; Castellani, F.; Garinei, A.; Astolfi, D.; Piccioni, E.; Desideri, U.; Vuillermoz, E. On the Possible Wind Energy Contribution for Feeding a High Altitude Smart Mini Grid. *Energy Procedia* **2015**, *75*, 1072–1079. [CrossRef]
24. Hu, J.; Harmsen, R.; Crijns-Graus, W.; Worrell, E. Geographical Optimization of Variable Renewable Energy Capacity in China Using Modern Portfolio Theory. *Appl. Energy* **2019**, *253*, 113614. [CrossRef]
25. Freitas, M.; Soito, J. Vulnerability to Climate Change and Water Management: Hydropower Generation in Brazil. *WIT Trans. Ecol. Environ.* **2009**, *124*, 217–228. [CrossRef]
26. Hamududu, B.; Killingtveit, A. Assessing Climate Change Impacts on Global Hydropower. In *Climate Change and the Future of Sustainability*; Apple Academic Press: Point Pleasant, NJ, USA, 2017; pp. 109–132.
27. Spalding-Fecher, R.; Chapman, A.; Yamba, F.; Walimwipi, H.; Kling, H.; Tembo, B.; Nyambe, I.; Cuamba, B. The Vulnerability of Hydropower Production in the Zambezi River Basin to the Impacts of Climate Change and Irrigation Development. *Mitig. Adapt. Strateg. Glob. Change* **2016**, *21*, 721–742.
28. Van Vliet, M.; Van Beek, L.; Eisner, S.; Flörke, M.; Wada, Y.; Bierkens, M.F.P. Multi-Model Assessment of Global Hydropower and Cooling Water Discharge Potential under Climate Change. *Glob. Environ. Change* **2016**, *40*, 156–170. [CrossRef]
29. Pokhrel, Y.N.; Oki, T.; Kanae, S. A Grid Based Assessment of Global Theoretical Hydropower Potential. *Proc. Hydraul. Eng.* **2008**, *52*, 7–12. [CrossRef]
30. Fan, J.-L.; Hu, J.-W.; Zhang, X.; Kong, L.S.; Li, F.; Mi, Z. Impacts of Climate Change on Hydropower Generation in China. *Math. Comput. Simul.* **2020**, *167*, 4–18. [CrossRef]
31. Lehner, B.; Czisch, G.; Vassolo, S. The Impact of Global Change on the Hydropower Potential of Europe: A Model-Based Analysis. *Energy Policy* **2005**, *33*, 839–855. [CrossRef]
32. Wang, B.; Liang, X.-J.; Zhang, H.; Wang, L.; Wei, Y. Vulnerability of Hydropower Generation to Climate Change in China: Results Based on Grey Forecasting Model. *Energy Policy* **2014**, *65*, 701–707. [CrossRef]
33. Gaudard, L.; Romerio, F. Reprint of "the Future of Hydropower in Europe: Interconnecting Climate, Markets and Policies". *Environ. Sci. Policy* **2014**, *43*, 5–14. [CrossRef]
34. Ruggiero, S.; Lehkonen, H. Renewable Energy Growth and the Financial Performance of Electric Utilities: A Panel Data Study. *J. Clean. Prod.* **2017**, *142*, 3676–3688. [CrossRef]
35. Boehlert, B.; Strzepek, K.M.; Gebretsadik, Y.; Swanson, R.; McCluskey, A.; Neumann, J.; McFarland, J.; Martinich, J. Climate Change Impacts and Greenhouse Gas Mitigation Effects on Us Hydropower Generation. *Appl. Energy* **2016**, *183*, 1511–1519. [CrossRef]
36. De Lucena, A.F.P.; Szklo, A.S.; Schaeffer, R.; Souza, R.R.; Borba, B.; Costa, I.; Pereira, A.O., Jr.; Cunha, S.H.F. The Vulnerability of Renewable Energy to Climate Change in Brazil. *Energy Policy* **2009**, *37*, 879–889. [CrossRef]

37. REN21. *Renewables 2017 Global Status Report*; REN21 Secretariat: Paris, France, 2017.
38. World Energy Council. *World Energy Council Annual Report 2021*; World Energy Council: London, UK, 2021.
39. Hueging, H.; Haas, R.; Born, K.; Jacob, D.; Pinto, J.G. Regional Changes in Wind Energy Potential over Europe Using Regional Climate Model Ensemble Projections. *J. Appl. Meteorol. Climatol.* **2013**, *52*, 903–917. [CrossRef]
40. Peter, J. How Does Climate Change Affect Electricity System Planning and Optimal Allocation of Variable Renewable Energy? *Appl. Energy* **2019**, *252*, 113397. [CrossRef]
41. Carvalho, D.; Rocha, A.; Gómez-Gesteira, M.; Santos, C.S. Potential Impacts of Climate Change on European Wind Energy Resource under the CMIP5 Future Climate Projections. *Renew. Energy* **2017**, *101*, 29–40. [CrossRef]
42. Cradden, L.C.; Harrison, G.P.; Chick, J.P. Will Climate Change Impact on Wind Power Development in the UK? *Clim. Change* **2012**, *115*, 837–852. [CrossRef]
43. Solaun, K.; Cerdá, E. Impacts of Climate Change on Wind Energy Power–Four Wind Farms in Spain. *Renew. Energy* **2020**, *145*, 1306–1316.
44. Dupont, E.; Koppelaar, R.; Jeanmart, H. Global Available Wind Energy with Physical and Energy Return on Investment Constraints. *Appl. Energy* **2018**, *209*, 322–338. [CrossRef]
45. Davidson, M.R.; Zhang, D.; Xiong, W.; Zhang, X.; Karplus, V.J. Modelling the Potential for Wind Energy Integration on China's Coal-Heavy Electricity Grid. *Nat. Energy* **2016**, *1*, 1–7.
46. Sherman, P.; Chen, X.; Mcelroy, M.B. Wind-generated Electricity in China: Decreasing Potential, Inter-annual Variability and Association with Changing Climate. *Sci. Rep.* **2017**, *7*, 16294. [PubMed]
47. Feng, J.; Feng, L.; Wang, J.; King, C. Evaluation of the Onshore Wind Energy Potential in Mainland China-Based on GIS Modeling and EROI Analysis. *Resour. Conserv. Recycl.* **2020**, *152*, 104484.
48. Hou, G.; Sun, H.; Jiang, Z.; Pan, Z.; Wang, Y.; Zhang, X.; Zhao, Y.; Yao, Q. Life Cycle Assessment of Grid-Connected Photovoltaic Power Generation from Crystalline Silicon Solar Modules in China. *Appl. Energy* **2016**, *164*, 882–890. [CrossRef]
49. MEE (Ministry of Ecology and Environment of the People's Republic of China). *First Biennial Update Report on Climate Change of the People's Republic of China*; Ministry of Ecology and Environment of the People's Republic of China: Beijing, China, 2017.
50. CMA (China Meteorological Administration). *2015 Annual Report on Wind and Solar Energy Resources in China*; Wind and Solar Energy Resource Center of CMA: Beijing, China, 2016.
51. Burnett, D.; Barbour, E.; Harrison, G.P. The UK solar energy resource and the impact of climate change. *Renew. Energy* **2014**, *71*, 333–343. [CrossRef]
52. Yushchenko, A.; De Bono, A.; Chatenoux, B.; Patel, M.K.; Ray, N. GIS-Based Assessment of Photovoltaic (PV) and Concentrated Solar Power (CSP) Generation Potential in West Africa. *Renew. Sustain. Energy Rev.* **2018**, *81*, 2088–2103. [CrossRef]
53. Merrouni, A.A.; Elalaoui, F.E.; Mezrhab, A.; Mezrhab, A.; Ghennioui, A. Large Scale Pv Sites Selection by Combining Gis and Analytical Hierarchy Process. Case Study: Eastern Morocco. *Renew. Energy* **2018**, *119*, 863–873. [CrossRef]
54. Aly, A.; Jensen, S.S.; Pedersen, A.B. Solar Power Potential of Tanzania: Identifying CSP and PV Hot Spots through a GIS Multicriteria Decision Making Analysis. *Renew. Energy* **2017**, *113*, 159–175. [CrossRef]
55. Siala, K.; Stich, J. Estimation of the Pv Potential in Asean with a High Spatial and Temporal Resolution. *Renew. Energy* **2016**, *88*, 445–456. [CrossRef]
56. Mondal, M.A.H.; Islam, A.S. Potential and Viability of Grid-Connected Solar Pv System in Bangladesh. *Renew. Energy* **2011**, *36*, 1869–1874. [CrossRef]
57. Gaetani, M.; Huld, T.; Vignati, E.; Monforti-Ferrario, F.; Dosio, A.; Raes, F. The near future availability of photovoltaic energy in Europe and Africa in climate-aerosol modeling experiments. *Renew. Sustain. Energy Rev.* **2014**, *38*, 706–716. [CrossRef]
58. Liu, J.; Xu, F.; Lin, S. Site Selection of Photovoltaic Power Plants in a Value Chain Based on Grey Cumulative Prospect Theory for Sustainability: A Case Study in Northwest China. *J. Clean. Prod.* **2017**, *148*, 386–397. [CrossRef]
59. Yang, Q.; Huang, T.; Wang, S.; Li, J.; Dai, S.; Wright, S.; Wang, Y.; Peng, H. A GIS-Based High Spatial Resolution Assessment of Large-Scale PV Generation Potential in China. *Appl. Energy* **2019**, *247*, 254–269.
60. He, G.; Kammen, D.M. Where, When and How Much Solar Is Available? A Provincial-Scale Solar Resource Assessment for China. *Renew. Energy* **2016**, *85*, 74–82. [CrossRef]
61. Chen, F.; Yang, Q.; Zheng, N.; Wang, Y.; Huang, J.; Xing, L.; Li, J.; Feng, S.; Chen, G.; Kleissl, J. Assessment of Concentrated Solar Power Generation Potential in China Based on Geographic Information System (GIS). *Appl. Energy* **2022**, *315*, 119045. [CrossRef]
62. Chen, S.; Lu, X.; Miao, Y.; Deng, Y.; Nielsen, C.P.; Elbot, N.; Wang, Y.; Logan, K.G.; McElroy, M.B.; Hao, J. The Potential of Photovoltaics to Power the Belt and Road Initiative. *Joule* **2019**, *3*, 1895–1912. [CrossRef]
63. Gernaat, D.E.; De Boer, H.S.; Daioglou, V.; Yalew, S.G.; Müller, C.; Vuuren, D.P. Climate Change Impacts on Renewable Energy Supply. *Nat. Clim. Change* **2021**, *11*, 119–125. [CrossRef]
64. Hoogwijk, M.M. On the Global and Regional Potential of Renewable Energy Sources. Ph.D. Thesis, Utrecht University, Utrecht, The Netherlands, 2004.

65. Gernaat, J.H.E.D.; Bogaart, W.P.; Vuuren, V.P.D.; Biemans, H.; Niessink, R. High-resolution assessment of global technical and economic hydropower potential. *Nat. Energy* **2017**, *2*, 821–828. [CrossRef]
66. Li, Y.; Chou, J.; Zhao, W.; Jin, H.; Guo, H. Development potential and carbon emission reduction effect of photovoltaics in countries along the belt and road. *Renew. Energy* **2026**, *256*, 123837.
67. Qiu, T.; Wang, L.; Lu, Y.; Zhang, M.; Qin, W.; Wang, S.; Wang, L. Potential Assessment of Photovoltaic Power Generation in China. *Renew. Sustain. Energy Rev.* **2022**, *154*, 111900. [CrossRef]

Disclaimer/Publisher's Note: The statements, opinions and data contained in all publications are solely those of the individual author(s) and contributor(s) and not of MDPI and/or the editor(s). MDPI and/or the editor(s) disclaim responsibility for any injury to people or property resulting from any ideas, methods, instructions or products referred to in the content.